

*Formula derivation for estimating natural frequency of  
anticlastic shells*

composed by

**BOMPOTAS NIKOLAOS**

under the supervision of

**Dr.ir. P.C.J. Hoogenboom**

May 2017

## **PREFACE**

With the current, the results of the conducted research for the development of a formula to estimate the lowest natural frequency of anticlastic shells, are presented. The study entitled «Formula derivation for estimating natural frequency of anticlastic shells», was carried out in the Civil Engineering department of TU Delft during the period 17<sup>th</sup> of February, to 19<sup>th</sup> of May, 2017, and constituted the subject of my internship in the framework of my participation in Erasmus+ programme, as a student of the Civil Engineering department of the University of Patras.

After a brief introduction, the description of the problem can be found in Chapter 1. Proceeding, a basic theoretical background regarding the shell structures of interest is reviewed in Chapter 2. In Chapter 3, the finite-element modelling used for the analysis, is depicted, and the reasoning behind the data acquisition is explained. Thereafter, the analysis of the collected data shall follow in Chapter 4, where useful observations will be made for the upcoming derivation of the formula seen in Chapter 5. Next, the results of the solution will be evaluated in Chapter 6, while the validity limits will also be defined in the same. Finally, Chapter 7 will be consisted of the conclusions of the study and some recommendations.

I would like to thank my supervisor, Dr.ir. P.C.J. Hoogenboom, for his guidance during the project and for the opportunity he gave me to develop myself both academically and socially those 3 months in Delft. It was a great pleasure cooperating and exchanging ideas with him. Last but not least, special thanks belong to my parents for supporting my choices and providing me with all the supplies to make my dreams come true.

Nikolaos Bompotas

Delft, May 2017

# Contents

Preface.....	i
Abstract.....	v
1 INTRODUCTION.....	1
1.1 Aim of study.....	1
1.2 Problem.....	1
1.3 Objective.....	1
2 BACKGROUND/THEORY.....	2
2.1 Shell structures and plates.....	2
2.2 Membrane theory.....	2
2.3 Classification of shells.....	2
2.3.1 Thickness-curvature relation.....	3
2.3.2 Gaussian curvature.....	3
2.4 Anticlastic shells.....	4
3 FINITE-ELEMENT MODELLING & DATA ACQUISITION.....	5
3.1 Finite-element model.....	5
3.2 Data acquisition.....	9
4 DATA ANALYSIS.....	11
4.1 Introduction.....	11
4.2 Base formula.....	11
4.3 Influence of length.....	12
4.4 Influence of thickness.....	16
4.5 Influence of curvature.....	19
5 SOLUTION.....	22
5.1 Introduction.....	22
5.2 Phase 1.....	22
5.3 Phase 2.....	27
5.4 Derived formula.....	29
6 EVALUATION OF THE RESULTS & VALIDITY LIMITS.....	31
6.1 Visualisation of the result.....	31
6.2 Error assessment.....	32
6.3 Validity limits of the derived formula.....	33
7 CONCLUSIONS AND RECOMMENDATIONS.....	36
REFERENCES.....	37
APPENDIX A.....	38
APPENDIX B.....	41
APPENDIX C.....	46

## List of Figures

<b>Figure 2.1</b> Membrane stresses of shell element, Hoefakker and Blaauwendraad 2003 .....	2
<b>Figure 2.2</b> (a)Positive Gaussian curvature, (b) Zero Gaussian curvature and (c) Negative Gaussian curvature, Hoefakker and Blaauwendraad 2003.....	3
<b>Figure 3.1</b> Shell FEM with $k=0.2 \text{ m}^{-1}$ , $\ell=1.0 \text{ m}$ .....	6
<b>Figure 3.2</b> Shell FEM with $k=0.2 \text{ m}^{-1}$ , $\ell=10.0 \text{ m}$ .....	6
<b>Figure 3.3</b> Vibration mode with 1 belly.....	7
<b>Figure 3.4</b> Vibration mode with 4 bellies .....	7
<b>Figure 3.5</b> Vibration mode with 9 bellies .....	8
<b>Figure 3.6</b> Vibration mode with 16 bellies.....	8
<b>Figure 4.1</b> Base formula vs ANSYS data.....	12
<b>Figure 4.2</b> Error between base formula and ANSYS data .....	13
<b>Figure 4.3</b> Base formula accordance with ANSYS data in later lengths .....	13
<b>Figure 4.4</b> Frequency curves of multiple vibration mode shapes.....	14
<b>Figure 4.5</b> Tendencies of term $D$ explained.....	15
<b>Figure 4.6</b> Term $D$ .....	15
<b>Figure 4.7</b> Base formula and ANSYS frequency, along with their difference and the error between them, combined.....	16
<b>Figure 4.8</b> Influence of thickness on natural frequency.....	17
<b>Figure 4.9</b> Points of separation from base formula's curves and first peak occurrence .....	17
<b>Figure 4.10</b> Error curves for different thicknesses .....	18
<b>Figure 4.11</b> Term $D$ for different thicknesses.....	19
<b>Figure 4.12</b> Influence of curvature on natural frequency .....	19
<b>Figure 4.13</b> Error curves for different curvature values .....	21
<b>Figure 4.14</b> Term $D$ for different curvatures .....	21
<b>Figure 5.1</b> Predicting the length for which the error becomes greater than 5% for the first time ...	23
<b>Figure 5.2</b> Predicting the length for which a peak occurs for the first time.....	24
<b>Figure 5.3</b> Data points for term $D$ that belong in region $R_1$ .....	25
<b>Figure 5.4</b> Data points for term $D$ in region $R_1$ , plotted in dimensionless quantities.....	25
<b>Figure 5.5</b> Surface fit in region $R_1$ , displayed from different perspectives .....	26
<b>Figure 5.6</b> Data points for term $D$ in region $R_2$ .....	27
<b>Figure 5.7</b> Data points for term $D$ plotted in a dimensionless space .....	27
<b>Figure 5.8</b> Surface fit in region $R_2$ , displayed from different perspectives .....	28
<b>Figure 6.1</b> Accordance of derived formula with ANSYS data, for Case 2 with $t=0.005\text{m}$ .....	31
<b>Figure 6.2</b> Accordance of the derived formula with ANSYS data, for all cases with $t=0.005\text{m}$ .....	32
<b>Figure 6.3</b> Data points for minimal lengths in region $R_0$ that exceed the 10% error mark .....	34
<b>Figure 6.4</b> Alignment of data points in region $R_0$ with error about -10%.....	34

# List of Tables

**Table 3.1** Summary of data acquisition.....10  
**Table 4.1** Influence of curvature on natural frequency for  $l= 0.2$  m .....20  
**Table C1** Comparison of ANSYS and formula frequencies for Case 1. ....46  
**Table C2** Comparison of ANSYS and formula frequencies for Case 2.....48  
**Table C3** Comparison of ANSYS and formula frequencies for Case 3.....50  
**Table C4** Comparison of ANSYS and formula frequencies for Case 4.....51  
**Table C5** Comparison of ANSYS and formula frequencies for Case 5.....52  
**Table C6** Comparison of ANSYS and formula frequencies for Case 6.....53  
**Table C7** Comparison of ANSYS and formula frequencies for Case 7.....54

## ABSTRACT

In the herein study, the influence of various parameters on the natural frequency of saddle shaped shell structures is examined. The variables decided to be investigated are the length, the thickness and the curvature. The conducted research concentrates on thin, anticlastic curved panels made of steel and of equal length and curvature in both directions, in absence of twisting.

For this purpose, a total number of 1396 finite-element models are generated in ANSYS and the acquired data are imported in MATLAB for their numerical analysis. A series of figures is, then, being deployed to explain the tendencies of the natural frequency for every variable.

A notable observation is that frequency displays an analogous relation to thickness,  $t \sim f$ , whereby, increasing thickness results to increased frequency. This is not the case when the length is looked upon. As the length becomes larger, the lowest frequency shows irregularities with various local maxima to arise. What applies, though, in all the examined cases, is that length demonstrates a high effect on the frequency in minimal dimensions. On the contrary, curvature is found to have insignificant effect in the same region and until a certain point that depends on a combination of  $k$  and  $\ell$ . After this point, curvature has a main effect in frequency in an analogous manner as well.

Great to notice is that all those variables of interest correlate to each other rather well and in recognisable patterns, which can be described with simple equations. Therefore, it is highly advantageous to find the proper dimensionless quantities to work with, that would include the influences of the variables altogether.

These relations are discovered here and the final outcome is the derivation of a formula that can approximate the value of the lowest natural frequency for any given combination of length, thickness and curvature that comply with certain conditions.

The formula produced, can be collectively expressed by:

$$f = \sqrt{\frac{\pi^2 E t^2}{12(1-\nu^2)\rho \ell^4}} + a \sqrt{\frac{E k^2}{\rho \nu}} \quad (5.12)$$

where

$$a = \begin{cases} 0, & 3.0725(kt)^{0.2726} > k\ell \\ \ln b_1, & 3.0725(kt)^{0.2726} < k\ell < 4.379(kt)^{0.2329} \\ e^{b_2}, & 4.379(kt)^{0.2329} < k\ell \end{cases} \quad (5.13)$$

and

$$\begin{cases} b_1 = 1.1679 + 0.0028e^{k\ell} - 0.1719e^{kt} \\ b_2 = -2.7953 - 0.0686e^{k\ell} + 0.4674 \ln(kt) \end{cases} \quad (5.14)$$

In the current, the limits of validity for this formula are also investigated, setting as a permissible margin of error the 10% value. This can be described by,

$$\frac{1}{100} > kt > \frac{1}{3300} \quad \text{and} \quad 8.62(kt) \leq k\ell \leq 2.0 \quad (6.4)$$

where both the expressions should be fulfilled simultaneously. The formula is also applicable for the whole range of the thin shells,  $(1/30) > kt > (1/4000)$ , given that the condition for  $k\ell$  is fulfilled, but with the reduced accuracy of about 15%.

# 1 INTRODUCTION

## 1.1 Aim of study

Thin shell structures need to be analysed for buckling. This analysis needs to include shape imperfections, nonlinear material behaviour such as yielding of steel, cracking of reinforced concrete and geometrical nonlinear behaviour. The analysis is time consuming and requires considerable expertise of the analyst. Subsequent design improvements are even more time consuming.

Shell buckling often starts locally, for example, somewhere in a large free form shell. Suppose that a formula would exist that predicts the load factor at which any shell part would buckle. A contour plot could be made of the buckling load factor over the surface of a shell. It would quickly give an overview of where and how a shell design needs to be improved. Unfortunately, this formula does not exist as yet. For specific shapes such as cylinders and spheres much literature is available but this cannot be generalised to a formula for any curvature. It is believed that it is possible to develop this formula from a large number of finite element analysis of thin shell structures. It is also believed that this formula will not be too large and will be reasonably accurate.

The number of variables is very large. (length, thickness, curvature, Young's modulus, Poisson's ratio, surface loading, membrane forces, imperfections, etc.). These are too many variables to consider at the same time. In this project, the first three variables will only be considered. The buckling problem can be rewritten into a vibration problem, therefore, the effect of those variables on the natural frequency will be searched herein.

## 1.2 Problem

In previous projects a formula for the lowest natural frequency of curved panels which lies within a margin of error of 20% was developed:

$$f = \sqrt{\frac{\pi^2 E t^2}{12(1-\nu^2)\rho \ell^4} + [(k_{xx} + k_{yy})^2 + 4k_{xy}^2] \frac{E}{16\pi^2 \rho}} \quad (1.1)$$

This formula is suitable for various sizes, curvatures and loads. However, for the case of anticlastic shells, of opposite curvatures and without twist, this equation leads to

$$f = \sqrt{\frac{\pi^2 E t^2}{12(1-\nu^2)\rho \ell^4}} \quad (1.2)$$

The above expression does not include the curvature in it, which practically means that curvature does not contribute to the stiffness. Obviously, this is not in conformity with reality and leads to false estimations. Furthermore, the limits of the above formula are also not known.

## 1.3 Objective

Apparently, the current formula is not applicable for the case of saddle-shaped panels of interest. The main objective of the study is to come up with a correction to the existing formula, so that it can return sufficiently accurate estimations for the lowest natural frequency. The correction to be introduced should not be too complex, aiming for an appealing final result for the new formula. Once the formula is derived, an investigation in order to discover its validity limits, shall follow.

## 2 BACKGROUND/THEORY

### 2.1 Shell structures and plates

Before proceeding to any analysis and in order to be in a position to evaluate properly the results, some major remarks in the theory accompanied with shell structures have to be made. Shells are basically a generalized concept of plates. Plates can be defined as flat structures with their two lateral dimensions being many times larger than their third dimension, the normal to the plane of the plate. Plates can be described if their mid-surface, thickness and material properties are known. Shells are also defined by their middle plane, thickness and material properties. The difference between plates and shells is observed in their structural behavior. In-plane loads of plates generate in-plane membrane forces, and out-of-plane loads result to moments and transverse shear forces. Because of the middle surface of shells is curved, they can carry out-of-plane loads by in-plane membrane forces, which is not possible for plates. This behaviour is in accordance to the Membrane Theory.

### 2.2 Membrane theory

The membrane behaviour of shell structures, refers to the stress flow in a shell element that consists of in-plane normal and shear, which help transferring the loads to the supports. This is nicely illustrated in Figure 2.1. In thin shells, the component of a stress normal to the shell surface is negligible in comparison to the other internal stress components and, hence, can be neglected in the classical thin shell theories.

The ability of carrying the load only by in-plane stresses is closely related to the way in which membranes carry their load. Because the flexural rigidity is much smaller than the extensional rigidity, a membrane under external load mainly produces in-plane stresses. In case of shells, the external load also causes stretching or contraction of the shell as a membrane, without producing significant bending or local curvature changes. This behavior of shells can, therefore, be described by the Membrane Theory.

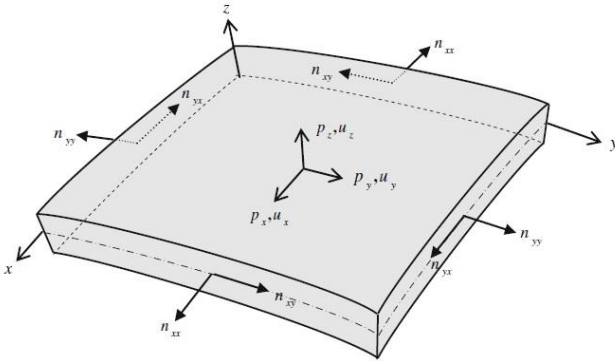


Figure 2.1 Membrane stresses of shell element, Hoefakker and Blaauwendraad 2003

### 2.3 Classification of shells

There are several ways the shells can be classified. Herein, only two of them will be discussed, as an attempt to demonstrate the basic characteristics of the curved panels of the current study. Those two classifications are referring to the thickness-curvature relation and the overall geometry of it.

### 2.3.1 Thickness-curvature relation

Depending on the analogy between the radius of curvature and the thickness, there are 4 different types to describe a shell:

- \* Very thick shell ( $r/t < 5$ ): which practically is not a shell due to its structural behaviour
- \* Thick shell ( $5 < r/t < 30$ ): which presents membrane forces as well as out of plane moments and out of plane shear forces
- \* Thin shell ( $30 < r/t < 4000$ ): which presents membrane forces as well as out of plane moments and out of plane shear forces, while, also, its bending stresses vary linearly over the thickness and the shear deformation can be neglected
- \* Membrane ( $4000 < r/t$ ): in which, all the loading is carried by membrane forces, while the out of plane bending moments and compressive forces are negligible

### 2.3.2 Gaussian curvature

For shell structures, it is convenient to make a classification according the Gaussian curvature. The Gaussian curvature of a three-dimensional surface is the product of the principal curvatures,  $k_1$  &  $k_2$ , which are defined as the maximum and minimum curvature of a certain surface. The principal curvatures can be found by intersecting a shell by an infinite number of planes normal to the shell surface at an arbitrary point and determining the two planes for which the secant with the surface has a maximum curvature and a minimum curvature. The principal curvatures are, by definition, orthogonal to each other. Because of this, it is convenient to take two axes of a local co-ordinate system on the surface along these principal sections. Taking a third axis normal to the surface at that point, yields an orthogonal three-dimensional co-ordinate system. The product of the principal curvatures

$$k_G = k_1 \cdot k_2 \quad (2.1)$$

provides the Gaussian curvature, which is either positive, zero or negative. Therefore, a classification depending on the Gaussian curvature means a classification in surfaces with positive Gaussian curvature (synclastic), zero Gaussian curvature (monoclastic) or negative Gaussian curvature (anticlastic), visualised in Figure 2.2.

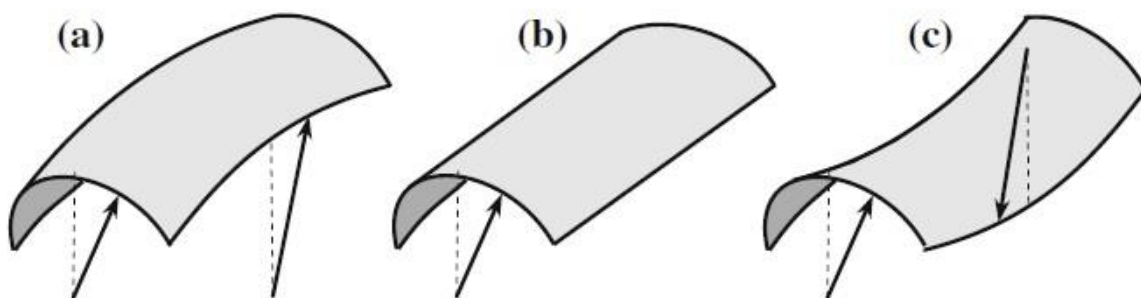


**Figure 2.2** (a) Positive Gaussian curvature, (b) Zero Gaussian curvature and (c) Negative Gaussian curvature, Hoefakker and Blaauwendraad 2003

## 2.4 Anticlastic shells

In the case of anticlastic shells, the two principal curvatures have opposite signs, which make the product negative. The characteristic feature of having a positive curvature in one direction and a negative curvature in the perpendicular direction, makes the shell act as a combination of a compression and tension arch when loaded perpendicular to its surface.

Anticlastic shells are often called hyper structures, which is a short way to describe their hyperbolic paraboloid shape. The analytical expression for defining the geometry of a hyper shallow shell of rectangular plan is

$$f(x, y) = \frac{1}{2}k_1x^2 - \frac{1}{2}k_2y^2 \quad (2.2)$$

A magnificent example of such structures is the largest aquarium in Europe, shown in Figure 2.3, which was designed by Félix Candela. Candela posited that “of all the shapes we can give to the shell, the easiest and most practical to build is the hyperbolic paraboloid”. This derives from the property of their shape, which can be defined by straight lines.



**Figure 2.3** L'Oceanogràfic, Valencia, Spain

### 3 FINITE-ELEMENT MODELLING & DATA ACQUISITION

#### 3.1 Finite-element model

According to the plan decided, the first step was to model different shells in a finite-element software and find the corresponding lowest natural frequency of each one. For this purpose, the ANSYS software was chosen to be used. Due to previous work and to the control someone can have over his model, the interface of the Mechanical APDL was selected, instead of the Workbench Mechanical. For purposes of easily modifying the values of the parameters, as well as of the frequency and the vibration mode shapes to be immediately displayed after the analysis, a script was used for the analysis. This was extremely efficient and led to saving precious time, which was eventually used for generating more models. The geometry input, the material used and the meshing were defined through this script which was read over and over again after the proper changes on the values of the variables. This script can be found in Appendix A.

The defined material had the following properties:

- \* Young's modulus:  $E = 210 \text{ GPa}$
- \* Poisson's ratio:  $\nu = 0.33$
- \* Density:  $\rho = 7850 \text{ kg/m}^3$

As far as the rest parameters used, the assumptions made for the focus area of this study, led to the introduction of:

- \*  $\ell_x = \ell_y = \ell$
- \*  $k_{xx} = -k_{yy} = k > 0$                       and                       $k_{xy} = 0$

Defining the model, it should be taken into account that an optimal selection for the meshing is of great significance. The elements used in the model, are of type shell181, which are suitable for the analysis of thin, to moderately thick shells. This type of elements is characterised by 4 nodes, each having 6 DOF- 3 translations and 3 rotations about the  $x$ ,  $y$  and  $z$  axes. For the modelling, a mesh with 50 elements in both the  $x$  – and  $y$  –directions has been selected in order to make the computations. This is already determined from the Bachelor Thesis of Ms. Greijmans [4], in which it was shown that an increase from 50 to 100 elements did not add considerable amount of accuracy. It was demonstrated that, for such a shaped panel, a number of 50 elements per direction, provided natural frequencies accurate enough to proceed. Besides, considering the total number of runs, an increase in the meshing density would be too time consuming.

Having optimised the mesh, the system of axes is rotated in each node, so that a local coordinate system is created. As a result, the forces are now acting in the direction of the shell member. The boundary conditions are defined as simple supports at all edges, leaving no freedom for perpendicular translations and, thus, eliminating the influences of the edges. In Figure 3.1 & 3.2, two shell examples of different curvatures and common length, are visualised.

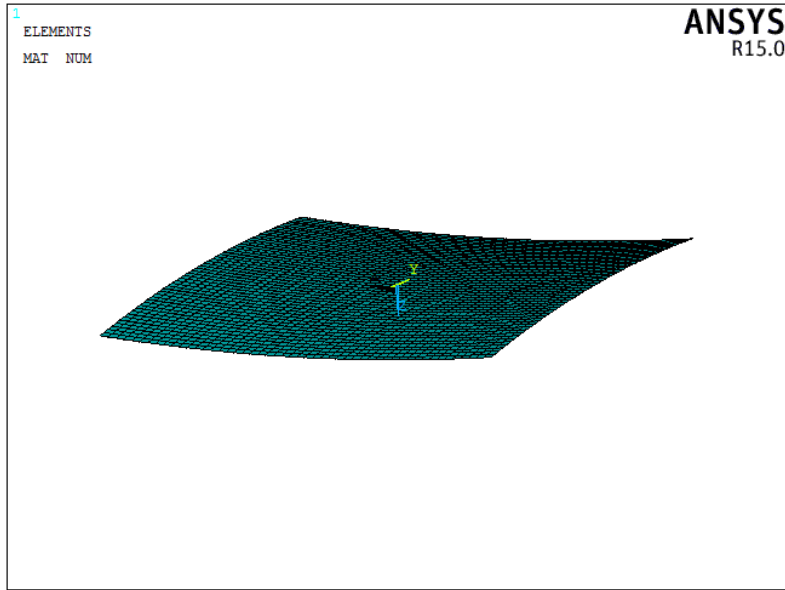


**Figure 3.1** Shell FEM with  $k=0.2 \text{ m}^{-1}$ ,  $\ell=1.0 \text{ m}$

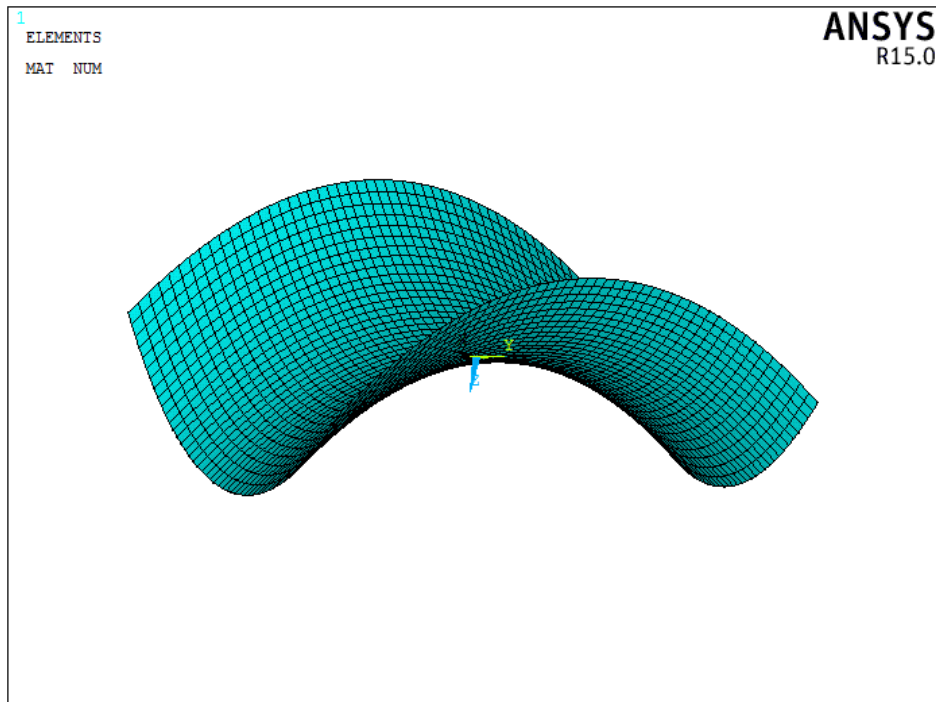


**Figure 3.2** Shell FEM with  $k=0.2 \text{ m}^{-1}$ ,  $\ell=10.0 \text{ m}$

It must be pointed out that the solution is not taking into consideration non-linear phenomena. Interested in conducting modal analysis, the script is written in such a way, so that ANSYS will return the calculated natural frequency of the dominant vibration mode, immediately after the solution. It is also requested to examine the vibration mode shapes corresponding to the lowest frequency, thus, a contour plot of the z- deformation is deployed, indicating the number of concavities emerge. In Figures 3.3-3.6 different vibration patterns are illustrated as displayed in ANSYS.

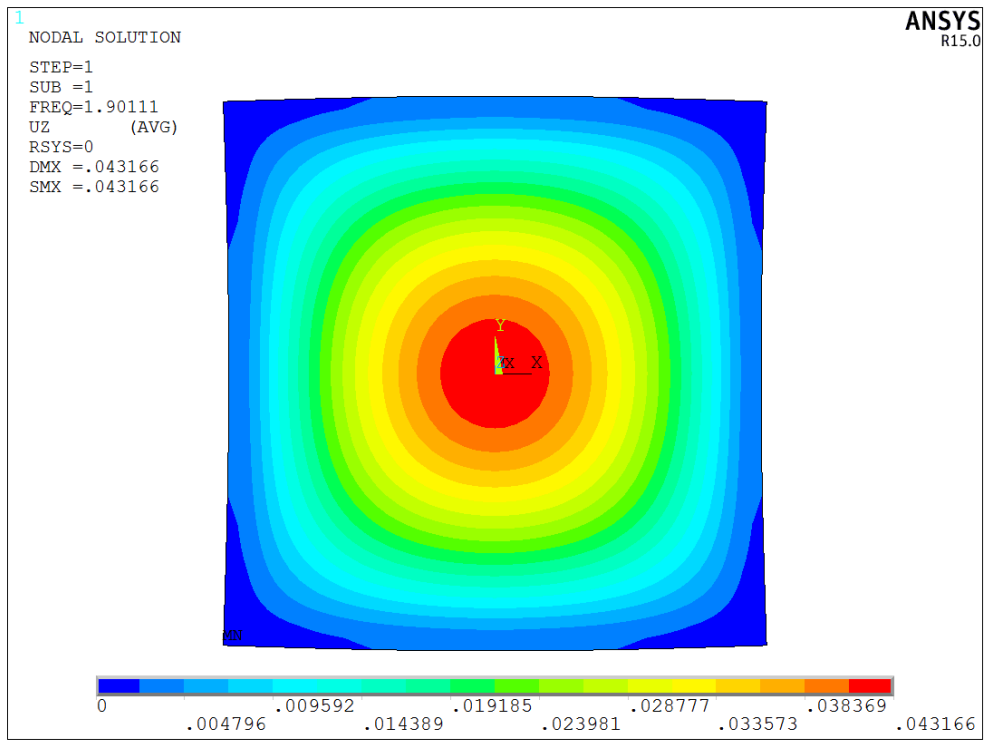


Figure 3.3 Vibration mode with 1 belly

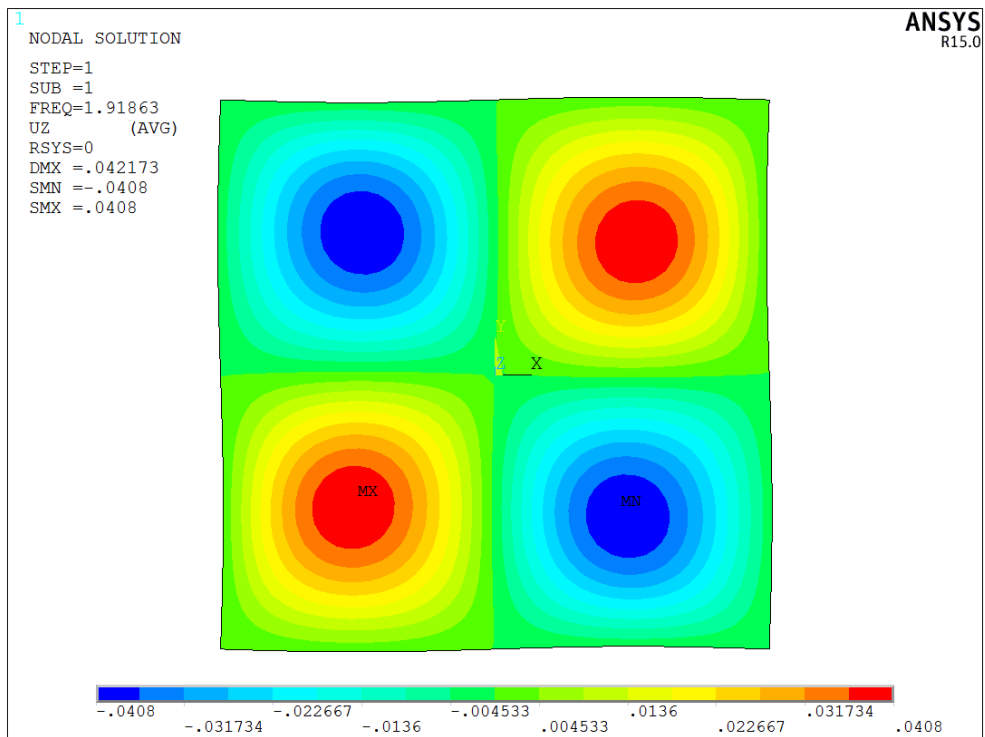


Figure 3.4 Vibration mode with 4 bellies

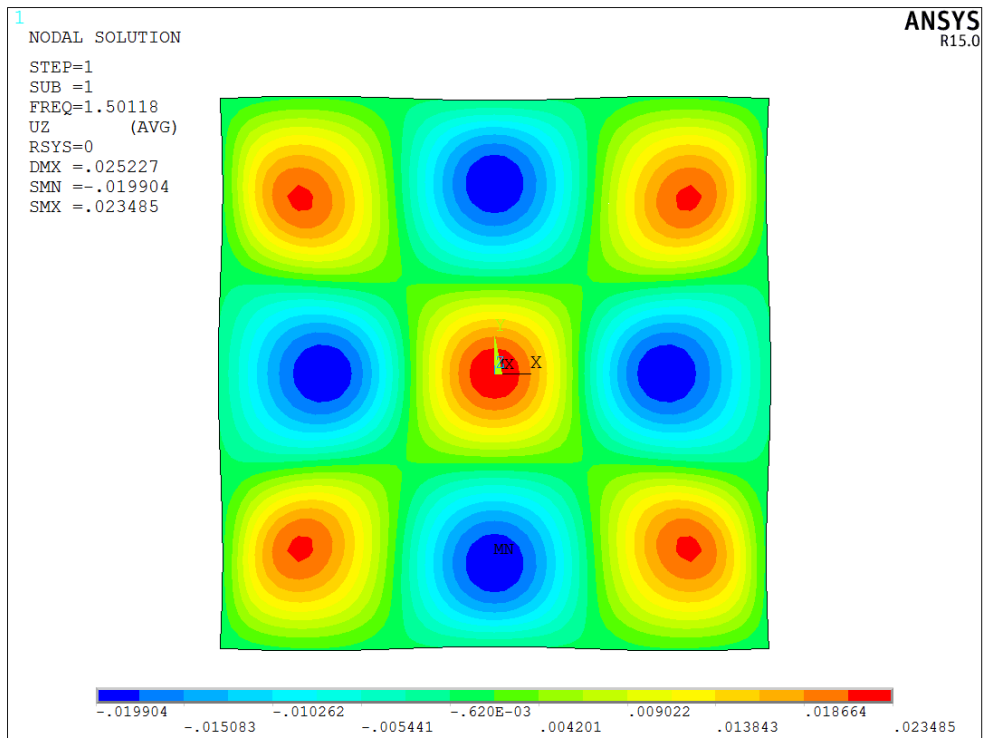


Figure 3.5 Vibration mode with 9 bellies

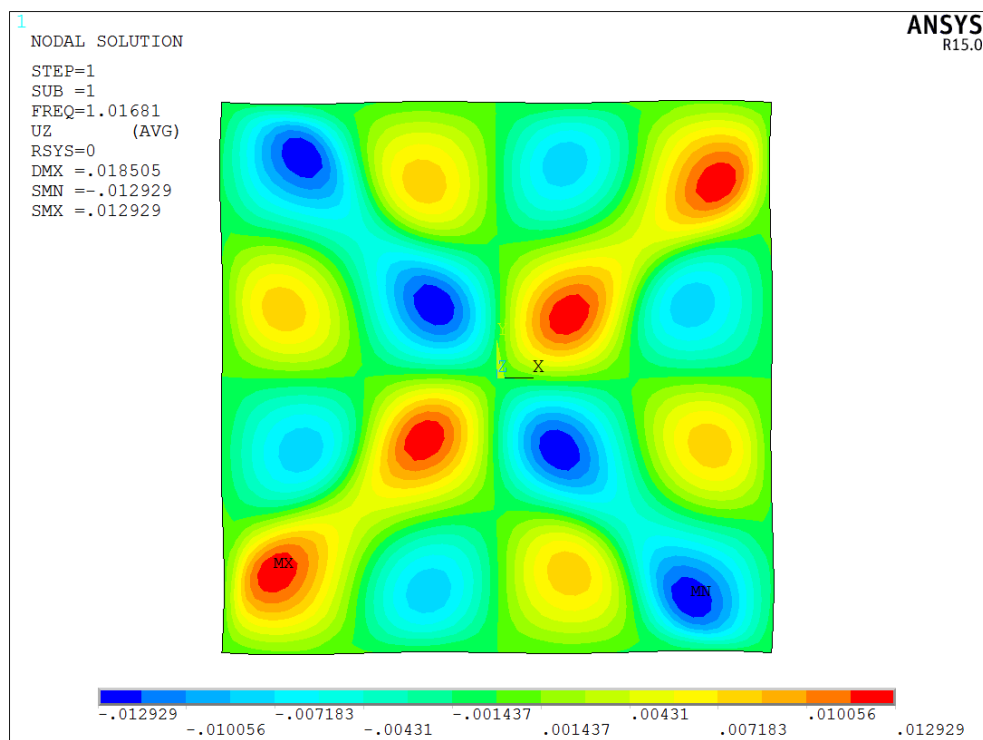


Figure 3.6 Vibration mode with 16 bellies

## 3.2 Data acquisition

Previous studies did not demonstrate a sufficient range of collected data, mainly due to the approach followed. Herein, the problem will be looked from a different standpoint. Instead of varying the values of the parameters without a specific syllogism, it was chosen to set boundaries according to certain assumptions. The concept behind the data acquisition was crucial for the final solution and the quality of the results and, therefore, it should be ascertained that the steps to the right direction were taken.

The approach was based on the main objective of parametric studies, recognising the importance of working with parametric dimensions, generating various configurations and refining the parameters, until satisfied with the results. Also, it is of great importance to identify the ranges of the parameters and specify the design constraints. Going forward, the range of the data acquisition is first defined. The study focuses on thin shells, so every generated model should comply with

$$30 < r/t < 4000 \quad (3.1)$$

or otherwise expressed,

$$(1/4000) < kt < (1/30) \quad (3.2)$$

As it can be observed, the panels shown in Figures 3.1 & 3.2, are two completely different cases despite having the same curvature value. This is because what matters the most is the analogy between the parameters. Trying to visualise how ‘curved’ a shell structure is, it is not enough to know only the curvature, but its combination with the length. For this reason, a relation correlating  $k$  &  $\ell$  is also introduced:

$$0 < k\ell \leq 2.0 \quad (3.3)$$

The upper limit of this condition was arbitrarily set as a goal value, mainly because of the shape of a panel with a combination of  $k$  and  $\ell$  of such a value. A panel characterised by  $k\ell = 2.0$ , can be seen in Figure 3.2.

As an attempt to obtain an organised set of data points, curvature was determined to vary in such a manner, that a realistic structure to exist. For example, if an extreme value  $k = 5 \text{ m}^{-1}$  was set, in order for the curvature to agree with the relations (3.2) & (3.3), the maximum value for the length variable would be  $\ell = 0.40 \text{ m}$ . while for the thickness would be  $t = 0.0067 \text{ m}$ , with the minimum reaching values  $t = 5 \cdot 10^{-5} \text{ m}$ . This is beyond the interests of this study, so the curvatures decided to be used were lying between

$$0 < k \leq 1.0 \quad (3.4)$$

Since there was a tendency in literature to focus mainly on smaller curvatures and being keen to investigate a different and wider range, the attention was paid to larger values, in the region of  $0.1 < k \leq 0.5$ , where more problems were arising. Other than that, data were collected for outlier values of the inequality (3.4), too.

Of course, the combinations are limitless, so a decision had to be made about the number of the models to be examined. The length was determined to be the variable with more dense variations, while for curvature there were 7 distinct cases, each one consisting of 4 subcases with different thicknesses. This is not a statistical analysis, so the number of lengths in each different case of curvature do not have to meet a certain condition. Having said that, there is a deviation between the number of models used in the 7 groups of data sets for the separate thicknesses. Overall, there were 1396 models analysed.

It has to be noticed, that the data acquisition was established in such a way, so that would assist the analysis followed. Looking ahead, the plan was to investigate the influence of every separate parameter on the natural frequency, isolated from the third variable each time. Consequently, in order for this to be achieved, and while thickness has numerous values that meet the condition (3.2), one common value can be observed in all the 7 different curvatures, corresponding to  $t = 0.005$  m.

All the data acquired can be found in Appendix C. Summarising, all the above discussed models are presented in short in Table 3.1.

Cases	1	2	3	4	5	6	7
$k$	0.05	0.10	0.20	0.30	0.40	0.50	1.00
$t$	<b>0.005</b>	0.0025	0.0015	0.001	0.001	0.001	0.0005
	0.010	<b>0.0050</b>	<b>0.0050</b>	<b>0.005</b>	<b>0.005</b>	<b>0.005</b>	0.001
	0.020	0.0100	0.0100	0.010	0.010	0.010	<b>0.005</b>
	0.050	0.0500	0.0500	0.050	0.050	0.050	0.010
Length Variations	80	100	50	34	25	20	40

**Table 3.1** Summary of data acquisition

## 4 DATA ANALYSIS

### 4.1 Introduction

In order to find the correlation between all the variables, the analysis of the collected data from the finite-element models seen in the previous Chapter, shall follow herein. It was very important to come up with an efficient approach for processing the data, because of the number of the parameters and the need for a rather simple result at the end. Before proceeding to the numerical analysis, it would be highly beneficiary to take a look at the influence of each of the variables on the lowest natural frequency of the shells of interest and acquire a better understanding of their behaviour. This will be achieved by a series of figures, where the tendencies of each term will be examined and compared to the results of the base formula, which was used as a starting point. The analysis was carried out with the help of MATLAB software.

### 4.2 Base formula

As it is already mentioned when stating the problem of the study, the currently available formula, given by eq. (1.1), does not work in the case of the anticlastic shells of interest. That's mainly because the curvature does not appear in it for the panels examined herein, something obviously wrong since it is seen to have significant effect in the frequency. Thus, the initial thought was to add a new term that would involve the missing curvature and maybe also the rest of the variables, length and thickness. As it was suggested in previous studies, this term should follow a parabolic trend which, indeed, sounded promising. Those recommendations, though, were not pointing to the right direction due to the fact they were focusing on small curvature values and on limited length and thickness variations. This led to conclusions useful only in a narrow spectrum, something that was in opposition to what was anticipated for the validity boundaries of the potential formula.

Nonetheless, a part of the current formula was decided to be retained and be used as a base of the new formula. The withheld part is given by eq. (1.2) and corresponds to the formula provided by Blevins, for calculating the exact value of the natural frequency of rectangular plates. More precisely, Blevins came up with the solution,

$$f_{ij} = \frac{\lambda_{ij}^2}{2\pi a^2} \sqrt{\frac{\pi^2 E h^3}{12\gamma(1-\nu^2)}} \quad (4.1)$$

where for a simply supported plate on all edges,

$$\lambda_{ij}^2 = \pi^2 \left[ i^2 + j^2 \left( \frac{a}{b} \right)^2 \right] \quad (4.2)$$

and

$a$  = length of plate

$b$  = width of plate

$h$  = thickness of plate

$i$  = number of half-waves in mode shape along horizontal axis

$j$  = number of half-waves in mode shape along vertical axis

$E$  = modulus of elasticity

$\gamma$  = mass per unit area of plate ( $\rho h$  for a plate of a material with density  $\rho$ )

$\nu$  = Poisson's ratio

This is a very promising starting point, especially if a closer look is taken at the general assumptions made in order to acquire the above expressions:

- The plates are flat and have constant thickness.
- The plates are composed of a homogenous, linear elastic, isotropic material.
- The plates are thin.

-The plates deform through flexural deformation. The deformations are small in comparison with the thickness of the plate. Normals to the midsurface of the undeformed plate remain straight and normal to the midplane during deformation. Rotary inertia and shear deformation are neglected.

- The in-plane load on the plates is zero.

Hence, many of the assumptions are in consonance with the herein research. It should be noted that, even though the study is not concentrating particularly on a vibration mode of one belly (corresponding to one half-wave along both the horizontal and vertical axes), the value used for the term  $\lambda_{ij}$  is given for  $i = 1$  and  $j = 1$ , despite the actual mode shape. It was chosen to overcome any difference caused by this, with the help of the term to be introduced later into the base formula.

### 4.3 Influence of length

In Figure 4.1, illustrated is the accordance between the chosen base formula and the results obtained from ANSYS using the example of a shell panel with curvature  $k = 0.10 \text{ m}^{-1}$  and thickness  $t = 0.005 \text{ m}$ . It can be noted that the selection of the Blevins' formula is a very sufficient starting point as it results to a concave up, decreasing curve that almost follows the course of the collected data.

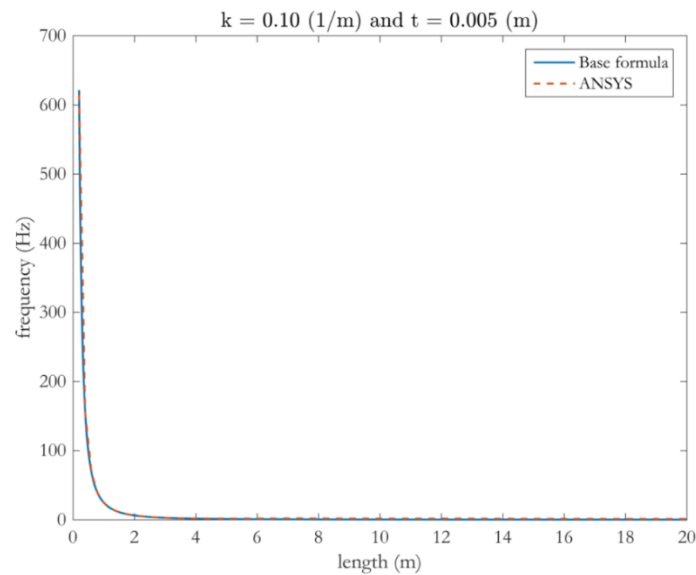


**Figure 4.1** Base formula vs ANSYS data

At first glance, someone may think the base formula does not need significant corrections. This, of course, would only be a careless mistake. For acquiring a better sense of the actual correspondence between the accurate frequency provided by the modelling in ANSYS and the one of the base formula, the margin error of those two quantities was examined. As it can be seen in Figure 4.2, the accordance is in admissible margins for the very first values of length, while from a point onwards it is becoming utterly intolerable. This is a key conclusion going forward.

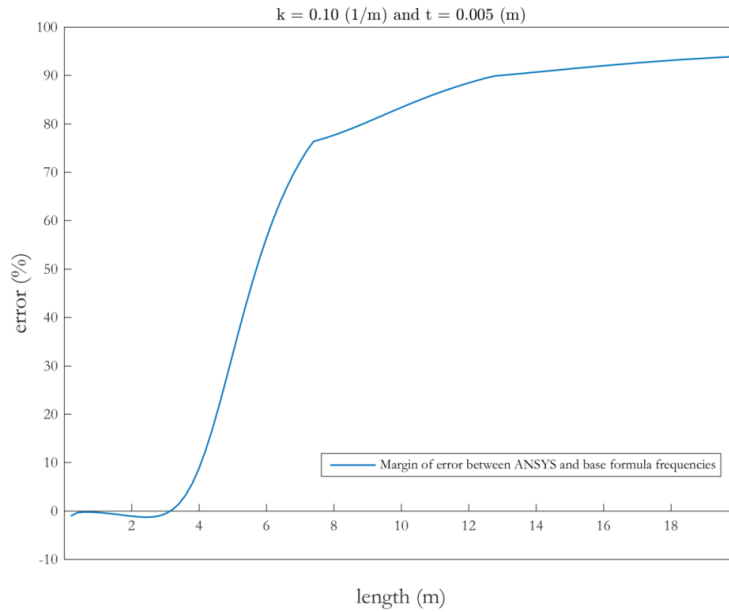


**Figure 4.2** Error between base formula and ANSYS data

The last observed frequency value to present an error lower than 5% associates to length  $\ell = 3.6$  m. Focusing on the region where the error is greater than 5%, results in Figure 4.3, which demonstrates the problems occurred when scaling Figure 4.1 and ignoring the first range of frequency values, where the base formula is found to be sufficiently accurate.

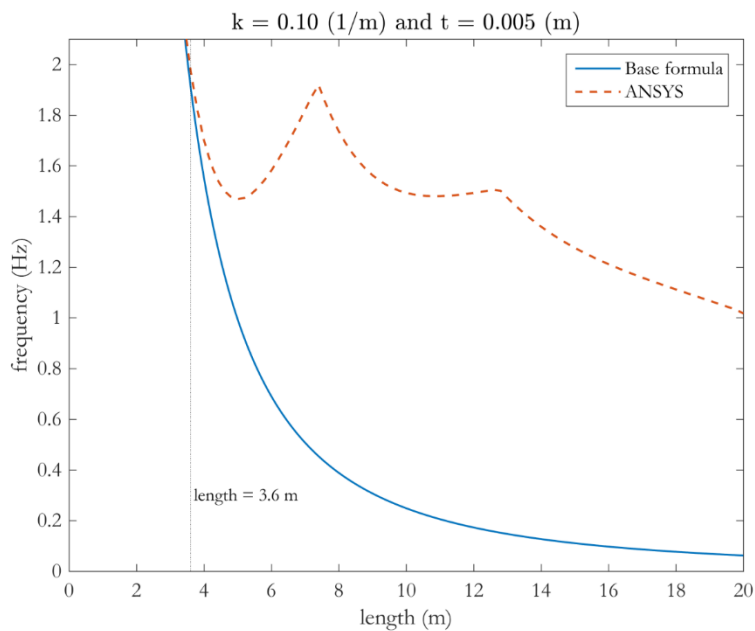


**Figure 4.3** Base formula accordance with ANSYS data in later lengths

It is clearly noticed that from this point onwards, the two curves diverge from each other. The peaks observed in the ANSYS data are completely normal and expected, standing for the points where a transition between different vibration patterns in the dominant vibration mode occurs. The first peak in the above Figure 4.3, represents a change in the first vibration mode shape, formerly constituting from 1 belly, shifting to a primary vibration mode shape of 4 bellies, while the second corresponds to the transition from 4 to 9 bellies. There is a third transition point from 9 to 16 bellies, which cannot be clearly

seen in this graph, as it coincides with the very last collected frequency for this shell panel and there is no peak going along with it, in the sense that no local maximum can be found as in the other two. This is not because there are no further data plotted after this point, but due to the location of the intersection point of the parabolas formed by the two different vibration patterns. For better understanding of this phenomenon, there were some more data acquired, exhibited in Figure 4.4.

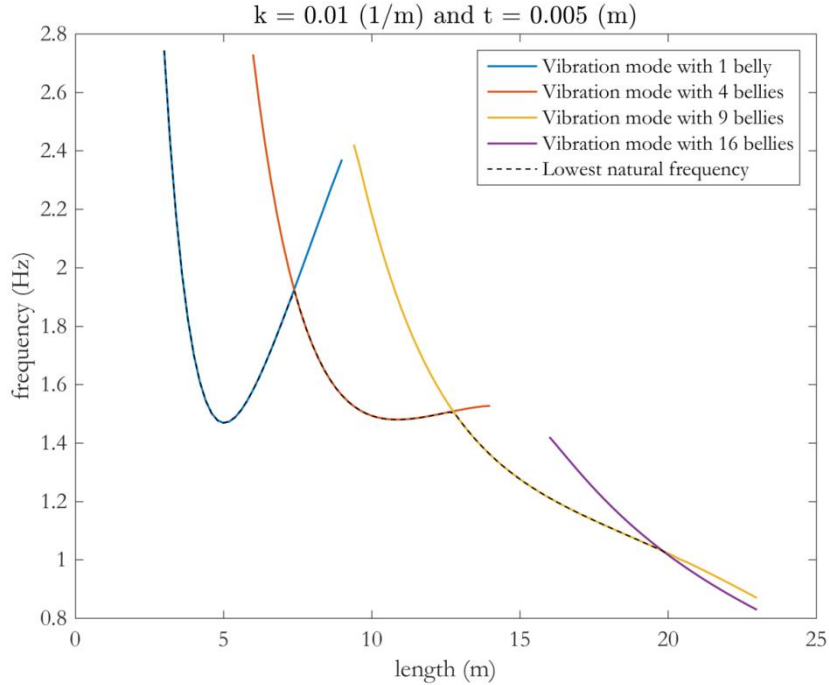


**Figure 4.4** Frequency curves of multiple vibration mode shapes

Each curve in Figure 4.4, associates to a particular vibration mode shape and represents the natural frequency of this mode for the indicative shell panel used herein. Varying the length, it can be observed that, after certain values, the lowest frequency corresponds to different vibration mode shapes. Here, being interested in those modes that are present in this study, only the cases of 1, 4, 9 and 16 bellies are displayed, but, of course, there is an infinite number of oscillation patterns. Attempting to estimate the lowest natural frequency and not the natural frequency which correlates to one particular vibration shape, results to the frequency curve that presents those tips. Moreover, there is another observation to be made on Figure 4.4, which will prove to be vital. The concavity of the parabolas shows a decreasing trend along with the change of the primary vibration mode shape, making it easier to approximate the curve of the lowest natural frequency in a simpler manner.

Going forward, the difference, introduced as  $D$ , between the frequency obtained from the finite-element model, from now on called ANSYS frequency, and the base formula, was examined:

$$D = f_{ANSYS} - f_b \quad (4.3)$$

Term  $D$  is expected to follow a 2-way trend in the focus area: increasing in the beginning and until the first peak occurs, whereby after this point, it should mainly descend, following, though, a compliant course to the ANSYS frequency curve. In the working example, the length for which the first transition between the vibration mode shapes emerges, is  $\ell = 7.4$  m. This results in two different areas of focus, presented visualised in the Figure 4.5 below.

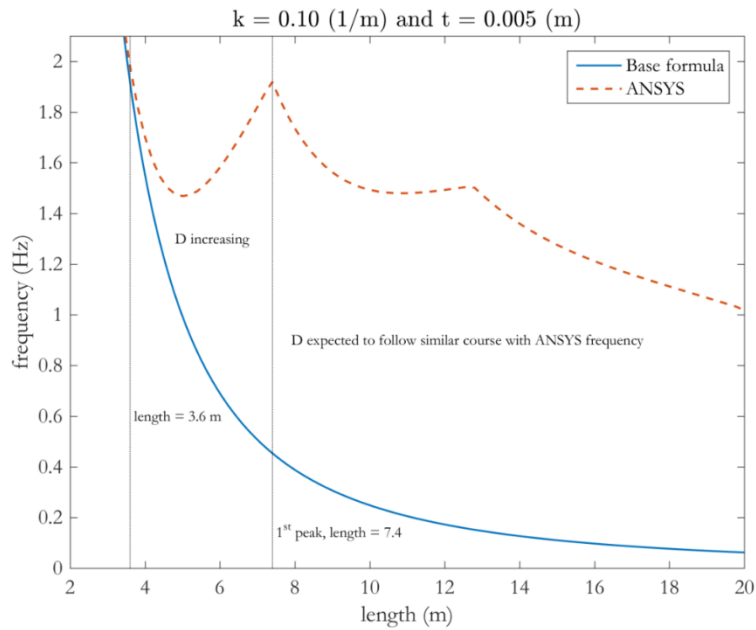


**Figure 4.5** Tendencies of term  $D$  explained

Indeed, plotting the difference against the length, produces Figure 4.6, where the tendencies of term  $D$  can be seen for each part. Not to be mistaken, the higher values of term  $D$  appearing in the region where  $\ell < 3.6$  m, do not indicate less accurate estimations from the base formula. This can be seen in combination with Figure 4.2, where the error can be observed that is displaying small values along the whole region.

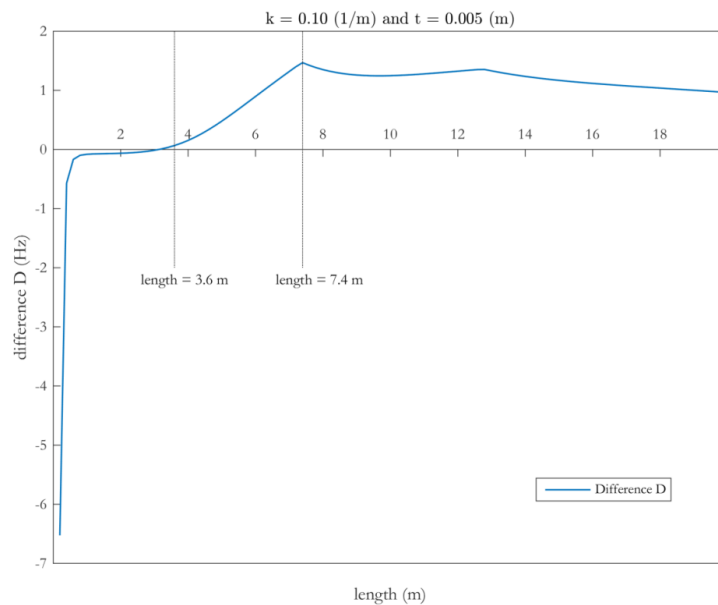


**Figure 4.6** Term  $D$

Avoiding confusions, in Figure 4.7, all terms of interest are plotted in one graph where all the above discussed details can be clearly seen, making it easier to comprehend how all those terms relate to each other and how the topic will be approached.

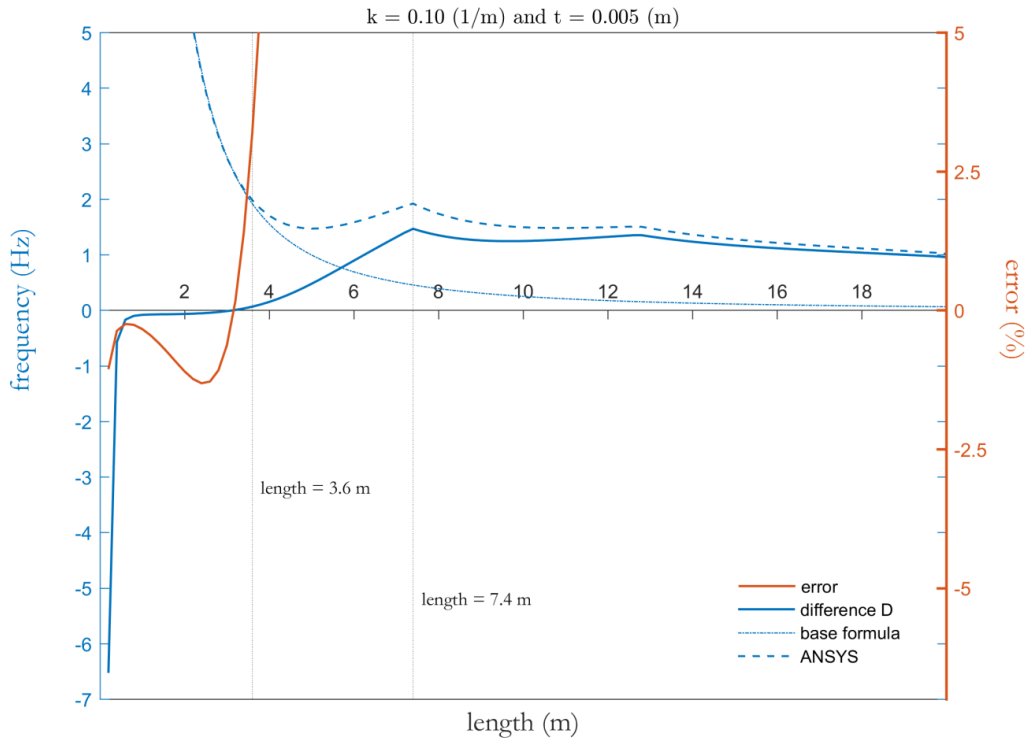


**Figure 4.7** Base formula and ANSYS frequency, along with their difference and the error between them, combined

#### 4.4 Influence of thickness

Interested in observing the variations in frequency provided by a change in the thickness variable, 4 data sets have been obtained for different values of it. Their respective graphs can be found in Figure 4.8. Evidently, the following safe conclusion can be drawn:

$$t \sim f \quad (4.4)$$

Contrarily with length, thickness demonstrates an analogous relation with frequency. Increasing or decreasing thickness, results to higher or smaller frequency values, respectively. In every subcase examined, the curve produced for a larger value of thickness is at all times above its preceding. Conveniently, enough, this is also the case for the curve produced by the base formula, which follows the movement of the curves provided by the data acquired.

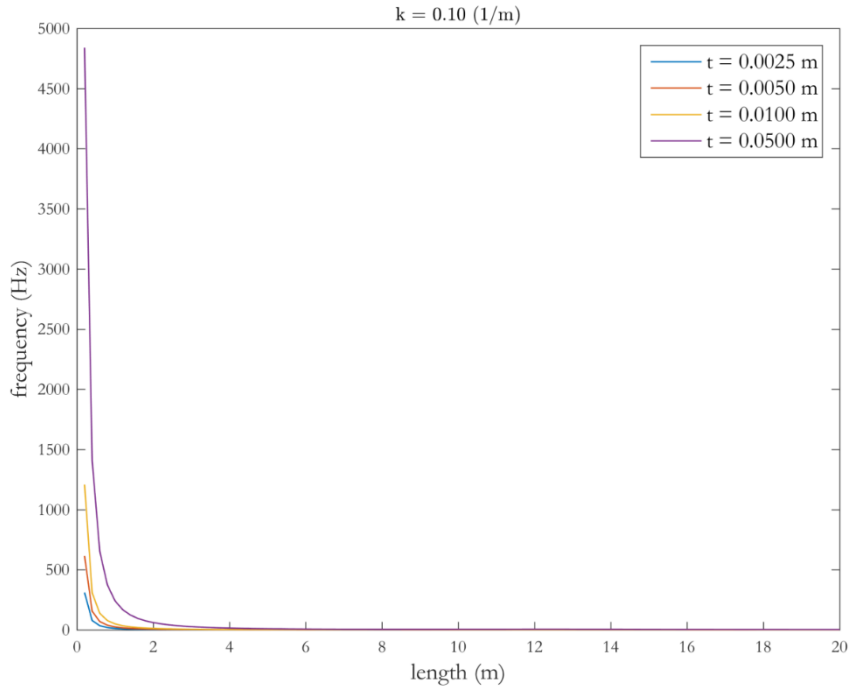


**Figure 4.8** Influence of thickness on natural frequency

What is also notable, is that along with the increase of thickness, the curves appear not only to rise, but move to the right side, too. This, has an inevitable consequence for the length for which the error becomes greater than 5% and the transition between the vibration mode shapes takes place, examined in the previous section. Figure 4.9, includes all those points for each separate curve, to illustrate their displacement in respect to thickness variance, and the tendency the latter shows.

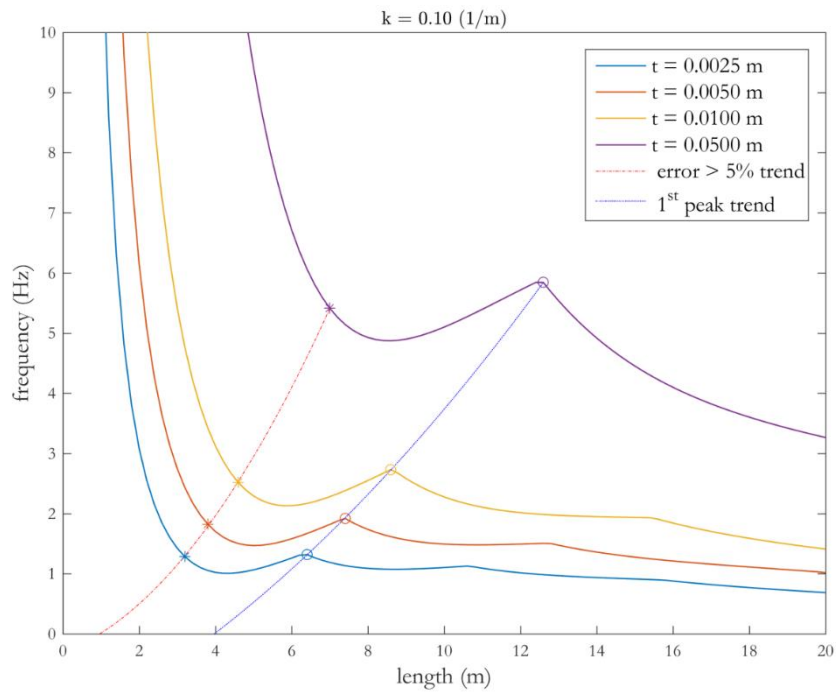


**Figure 4.9** Points of separation from base formula's curves and first peak occurrence

Proceeding to investigate the error between ANSYS frequency and the base formula, a complication is revealed. Displayed in Figure 4.10, error presents unacceptable values also for smaller lengths. In section 4.2, with the help of the working example with thickness  $t = 0.005\text{m}$ , it was showcased that for smaller lengths the error of prediction remained in sufficient margins. The explanation lies within the assumptions made in the first place, during the derivation of the used base formula. As it is already mentioned, this formula is valid for thin, flat plates. The troublesome behaviour appears for the lengths  $\ell = 0.020\text{ m}$  and  $\ell = 0.040\text{ m}$ , related to a panel with thickness  $t = 0.050\text{ m}$ . For this kind of lateral dimensions, such a panel is considered to be thick, since  $t > \ell/10$  applies. Nevertheless, this will be further discussed in section 4.5.

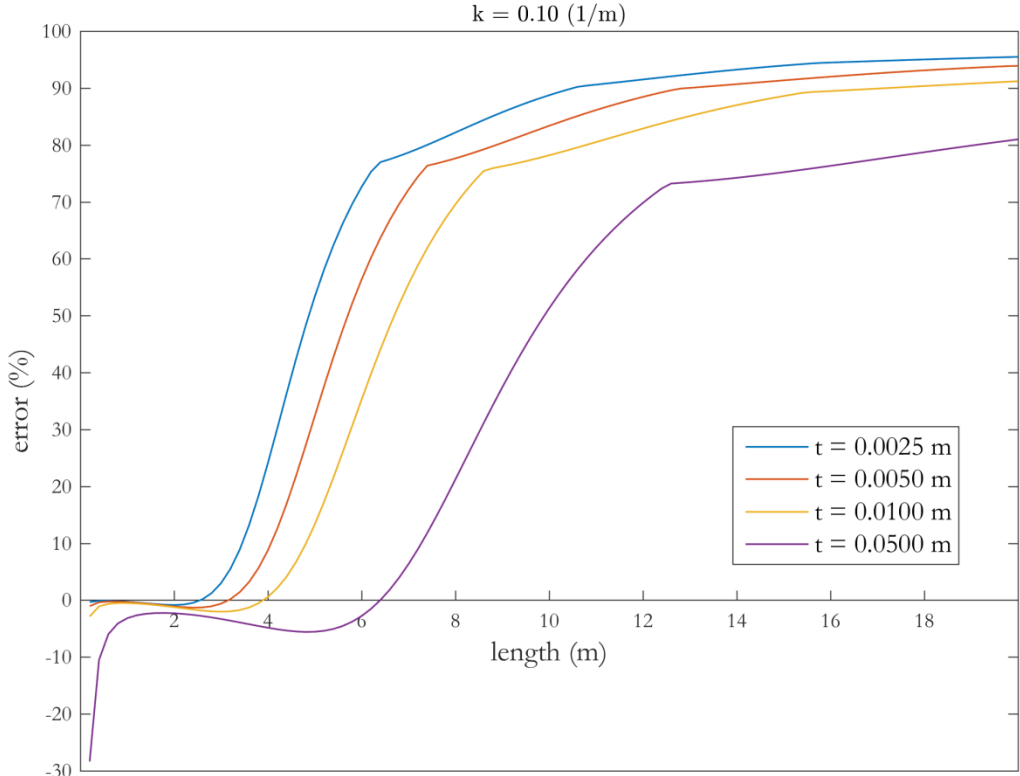


**Figure 4.10** Error curves for different thicknesses

Difference values are very useful to the approach followed, as they stand for the gap that needs to be covered so that the base formula can provide a sufficient approximation to the results of the finite-element models. Therefore, it is vital to observe tendencies of term  $D$  in respect to the herein variables. As it can be seen in Figure 4.11, despite the varying thickness, the curves retain their shape. This is a normal outcome due to the similar trajectories of the frequency curves displayed in Figures 4.8 & 4.9. An observation of great significance, though, is that all curves are well aligned in the region until the first peak is reached, with the exemption of the problematic subcase with  $t = 0.050\text{ m}$ . The part after the first peak is more complicated, constituting from several parabolic schemes in an interval manner which are not aligned, while at the same time, they are standing off a factor from each other.

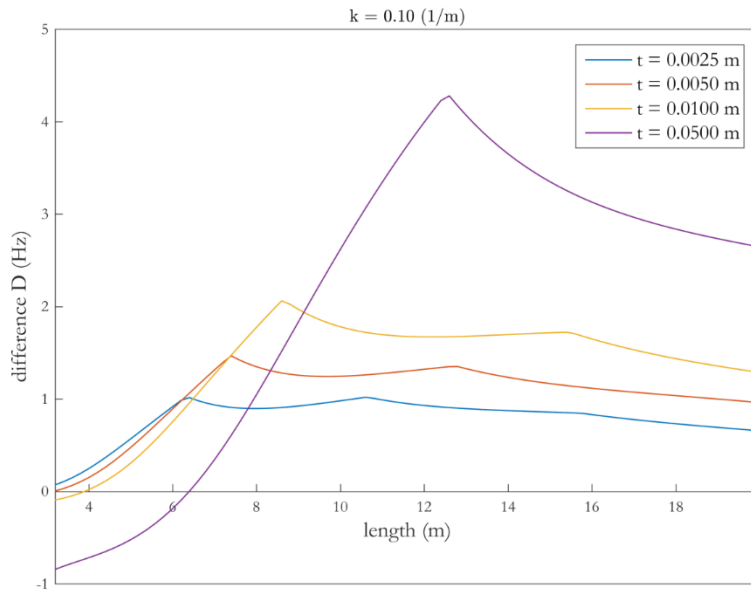


**Figure 4.11** Term  $D$  for different thicknesses

#### 4.5 Influence of curvature

Until this point, the influence of only two of the variables of interest was discussed. In this section, the reliance of the lowest natural frequency on the curvature, will be demonstrated using the data in possession of a total of seven distinct cases. For gaining a better understanding of the results, it is advised to isolate the influence of one of the other two parameters. It was selected to retain thickness at the same value for all those different cases and, therefore, the value  $t = 0.005$  m is purposely common to all the data sets acquired. Figure 4.12, has its y-axis in logarithmic scale resulting to a convenient visualisation of the whole range of values without interfering in the analogy between the curves. It can be quickly noticed that, curves corresponding to higher curvature values are located above the ones of smaller curvatures, indicating greater frequencies. This is not always the case, though.

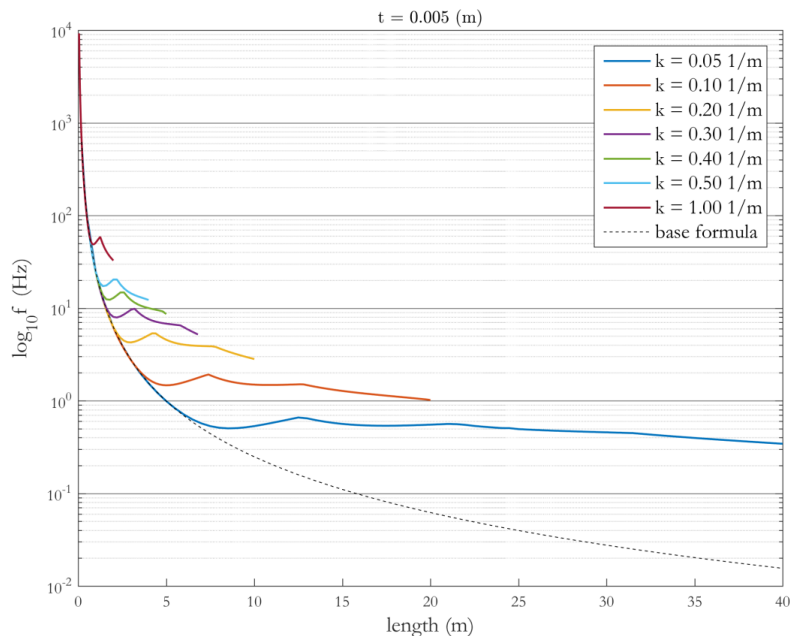


**Figure 4.12** Influence of curvature on natural frequency

Considering, for example, the case where  $\ell = 0.2$  m, demonstrated in Table 4.1 below, are the frequencies obtained from the finite-element models:

$k$ [ $\text{m}^{-1}$ ]	$f$ [Hz]
0.05	614.656
0.1	614.599
0.2	614.370
0.3	613.988
0.4	613.453
0.5	612.768
1.0	607.119

**Table 4.1** Influence of curvature on natural frequency for  $\ell=0.2$  m

Clearly, frequencies are almost equal to each other, but they also appear to decrease as the curvature increases. This is in contradiction to what has been seen happening at larger lengths. Nevertheless, the minimal dimensions where frequency displays the opposite trend than the aforementioned, are beyond the object of this study.

In the same graph, the curve of the base formula is also included. As curvature does not appear in this formula and thickness is not changing in the current section, only one curve transpires. What is of great significance, is that along the initial descending part of the curves, they all appear to substantially coincide. This basically means that, natural frequency is not significantly affected by curvature until a certain point and, therefore, can be accurately predicted by the base formula. For every case examined, the produced curve begins to separate from the one of the base formula when length exceeds a particular value, different for each case and depending on the curvature.

Another conclusion to be drawn from Figure 4.12 is that there is a variation of the number of peaks emerging inside the common boundary,  $k\ell \leq 2.0$ , set for this study. Shells with larger curvatures are characterized by higher sensitivity to length change when it comes to their eigen shape, subjecting to transition between vibration mode shapes in a quicker manner. Nonetheless, focusing on the range of interest, this transition occurs fewer times for larger values of curvature than in the smaller ones, making it more difficult to approximate all those different tendencies. Favourably, leaving the number of the transition points aside, there is a very promising tendency displayed by the locations of the first peaks, seemingly moving to the left and upwards to a possible recognisable pattern.

Concerning the error quantities, looking at Figure 4.13, there are no irregular incidences occurring, in the sense that they do not show any abnormalities as the one found in section 4.4. Based on the comment made therein, someone could argue that this is something unexpected, since the last case with  $k = 1.0 \text{ m}^{-1}$  gives a sufficient prediction that lies within 8% margin of error even in the small lateral dimensions examined. This is definitely an indication that curvature should be taken into consideration along with the rest of the parameters before coming to any relevant conclusions. In fact, this will play an important role in deciding the final boundaries of the validity of the formula. What is also observed, is that the slope of error curves is steeper for larger curvatures, showing a proneness to immediately develop intolerable values and, thus, being more sensitive to length change.

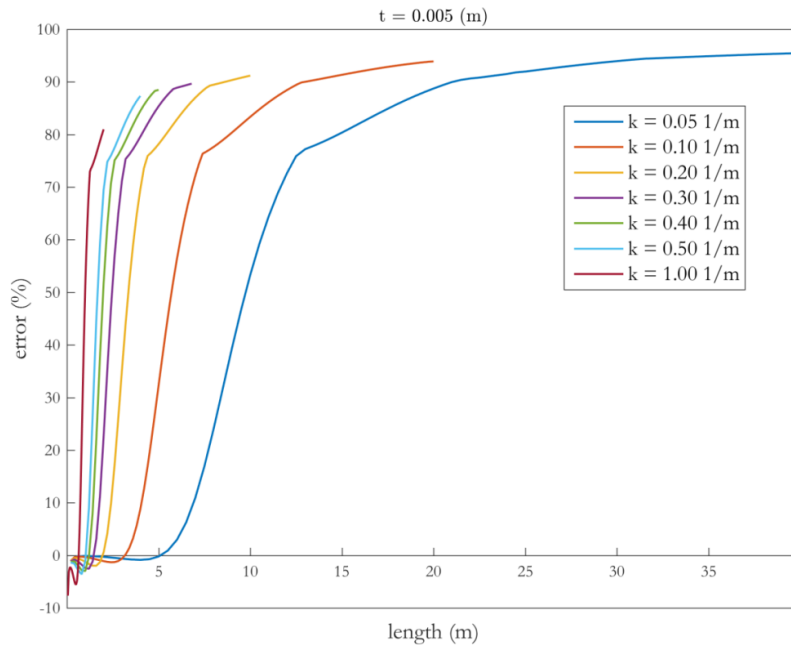


**Figure 4.13** Error curves for different curvature values

This is verified by Figure 4.14, where the difference values are represented for each case of the varied curvature. The reader must keep in mind that not all the values are plotted in this graph, but only those above -10 Hz, in an attempt to remain readable and suitable for rapid observations. Besides, with reference to Figure 4.13, these values are not of major importance. Concentrating on the area that needs to be corrected, it can be noticed that the difference follows the same pattern as already seen, with a primary increasing part, and a secondary, characterized by fluctuations, but mostly following a downward trend. The steeper slopes for larger curvatures indicate a susceptibility to a change in length, but the overall behaviour and shape are analogous for every case.

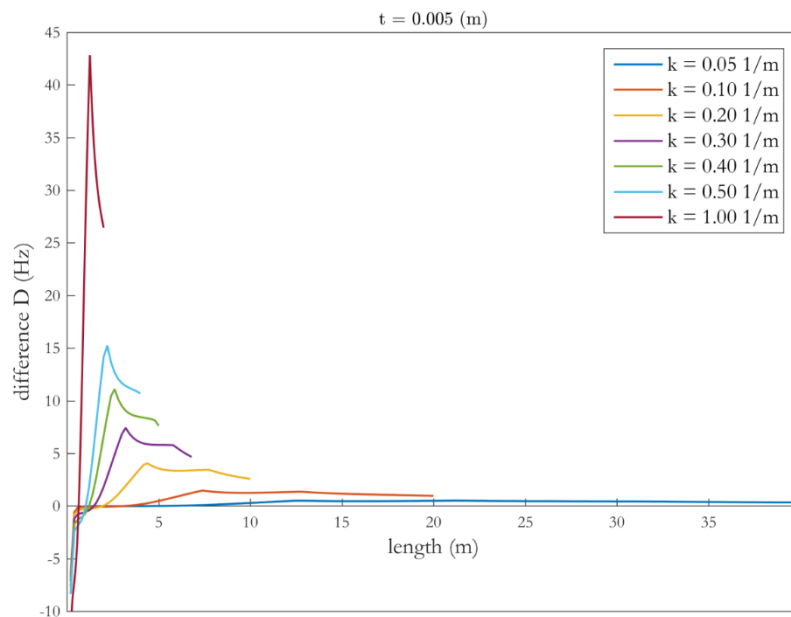


**Figure 4.14** Term  $D$  for different curvatures

## 5 SOLUTION

### 5.1 Introduction

The conceptual idea is to add a new term to the base formula, hereafter called  $C$ , so that the new formula produced, can estimate sufficiently the lowest natural frequency of a wide range of steel shell structures. Introducing term  $C$  as an added quantity outside the square root of base formula, leads to:

$$f = \sqrt{\frac{\pi^2 E t^2}{12(1-\nu^2)\rho \ell^4}} + C \quad (5.1)$$

Term  $C$  should not be too complex, as the formula would then lose its usability and is important to be easily manipulated further, helping the development of a shell buckling model. Also,  $C$  must be given in Hz units and be applicable to all cases. Due to the number of variables, this is better achievable working in dimensionless units. This provides various advantages, such as the inclusion of the influence of all the variables together, as well as the appliance of the valuable observations made in the previous chapter. The study will be consisted of the two upcoming parts: Phase 1, where an attempt will be made to approximate the values of the initial inclined part of the difference curves, starting from the point that presents error greater than 5% for the first time, and until the occurrence of the first peak, and Phase 2, where an estimation for the rest of the difference values after the first peak will be searched.

### 5.2 Phase 1

In the previous Chapter, a focus on the region where the error exceeds the positive 5% can be noted. This is a very satisfying starting point for the accuracy of the formula and was set as the condition for finding the points where the base formula requires a correction. Before this point, the accordance is adequate, except for some distinct values in extreme occasions, that fall out of the boundaries of the acceptable error in the negative side (over-prediction of base formula). This will be covered in Chapter 6, though. In Figure 4.9, it was demonstrated that the data points which present error amounts greater than 5% for the first time, when thickness was varied and curvature was retained steady, follow a somewhat parabolic trend when plotted against length. This happens to be also the case when the curvature varies and thickness remains the same. This can be seen in Figure 4.12, identifying the points where error is becoming greater than 5% as the spots in which the curves start to separate from the curve provided by the base formula. It would be very convenient if all those points could be predicted really accurately with a simple equation, taking into consideration the effect of all the variables at once. Therefore, a pattern which would connect the influence of curvature and thickness to the length, for which the aforementioned phenomena are observed, will have to be discovered. This relation is further sought here.

The key principle to find this relation, is hidden in the goal set in the beginning. There was a preference for the final formula to be valid for a wide range of structures that fulfil the assumptions made. For this purpose, it was decided that it would be highly advantageous to work with properly selected dimensionless quantities, instead of using the dimensional variables.

Summarising the above, as an attempt to isolate the effects of the third variable each time, only either curvature or thickness was changing, and the value of the length, for which, error has for the first time a value greater than 5%, was looked upon. This led to the introduction of the recognisable combination,  $kt$ , as the independent variable in the searched expression. Going back and recalling the limits set for the data acquisition, it can be seen that frequencies were collected inside a range of lengths, which was varying depending on the curvature, in respect to the relation  $k\ell \leq 2.0$ . This indicates that is

more reasonable to use the dimensionless quantity,  $k\ell$ , as the dependent term of the function to be derived.

A script that automatically finds all the errors meeting the condition  $\text{error} > 5\%$  for the first time, and stores the combination values of curvature-thickness,  $kt$ , and the dimensionless length,  $k\ell$ , for which they occur, was developed. Plotting the pairs of  $k\ell$  &  $kt$  results in the scattered data in Figure 5.1.

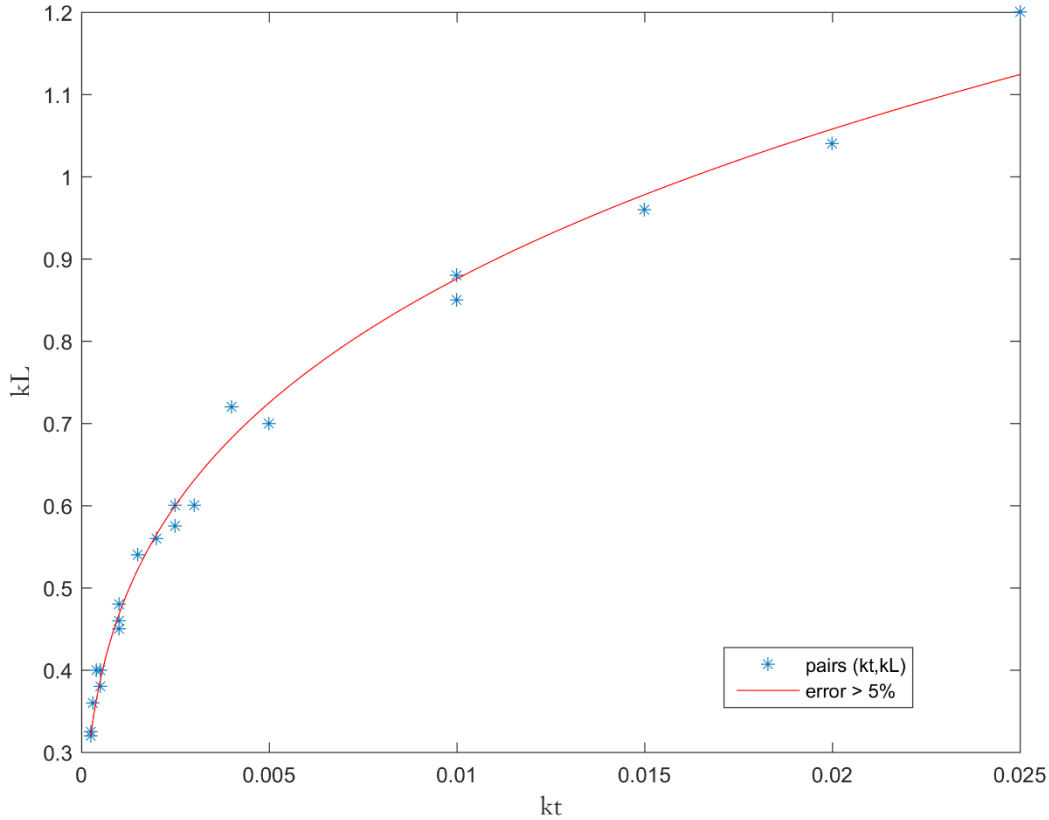


**Figure 5.1** Predicting the length for which the error becomes greater than 5% for the first time

In the above graph, the red curve represents the best fit to the data, which can be expressed as follows:

$$k\ell = 3.0725(kt)^{0.2726} \quad (5.2)$$

This power model fits very well the scattered points and an appearing gap between some of those points and the fitted curve can also be justified with the simple fact that frequencies in the collected data were not returning exactly a value of 5%. Therefore, there is a variation appearing depending on the density of the data acquired for each case, with the values closer to 5% being better adjusted to this curve. An optimisation can be made to improve the model by acquiring more data close to this set limit, but it is not being done herein and it is not believed that will influence the final result significantly. The above expression, eq. (5.2), estimates for every combination of  $k$  and  $t$ , the value of  $\ell$ , for which the base formula exceeds the error of 5%.

Interested in the ascending part of term  $D$ , it should now be examined where this incline discontinues. This point, corresponds to the location of the first peak in each curve, for all the different thicknesses and curvatures. An investigation was made of whether a simple equation could be derived, that would predict the ending point of the inclined difference part.

Following the same approach as earlier, a script was developed once again for locating the first peak, gathering the combination values of curvature-thickness,  $kt$ , and the dimensionless length,  $k\ell$ , for which they occur, as an attempt to relate all those points to each other. Plotting the obtained data, results to Figure 5.2.

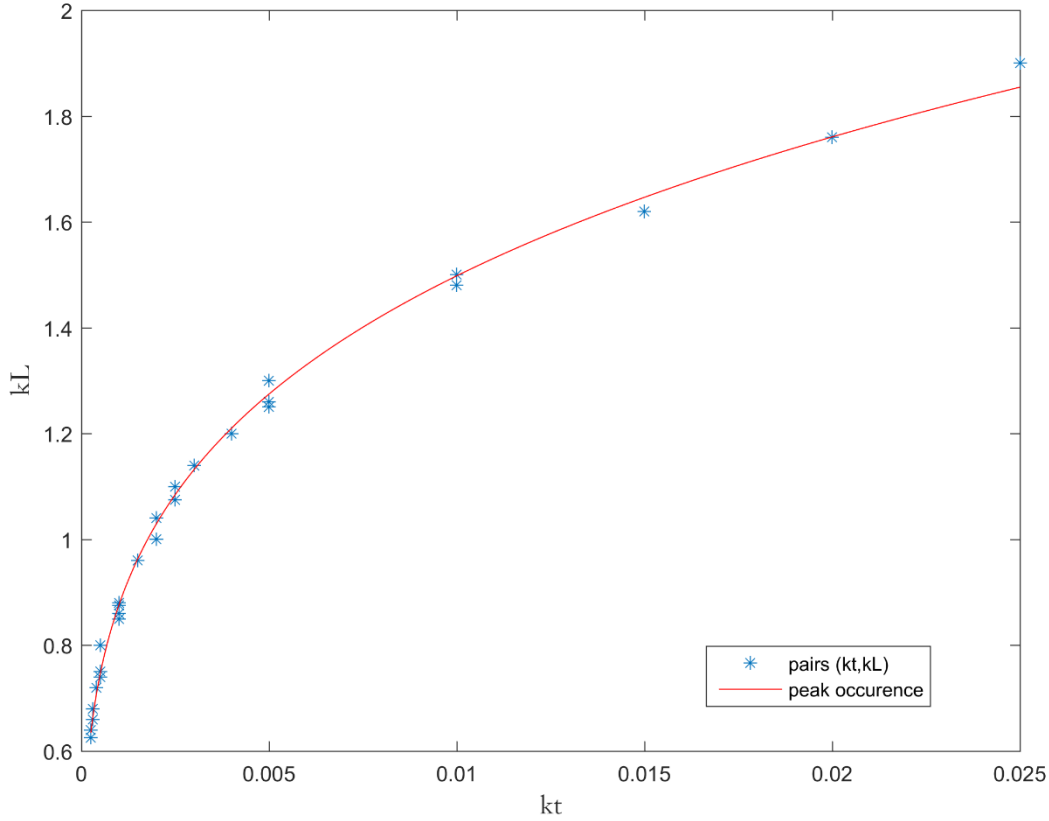


**Figure 5.2** Predicting the length for which a peak occurs for the first time

Conveniently, the data acquired display an also similar trend. The scattered points are fitted with the power model, given by:

$$k\ell = 4.379(kt)^{0.2329} \quad (5.3)$$

This equation returns the value of  $\ell$ , for which the upward tendency of the first examined part of difference term,  $D$ , ends, for every combination of  $k$  and  $t$ .

Based on the conclusions made in Chapter 4 regarding the analogy the difference curves are presenting, as well as the alignment they are displaying along the initial inclined part, an attempt of expressing term  $D$  for all cases in one, follows. Going forward, all  $D$  values for lengths that fall in the region hereafter called  $R_1$ , defined by the eq. (5.2) & (5.3), are collected and plotted in Figure 5.3. This figure visualises all those different points in a 3-D scattered plot, as an attempt to demonstrate the need to work with properly selected quantities that would limit their dispersion.

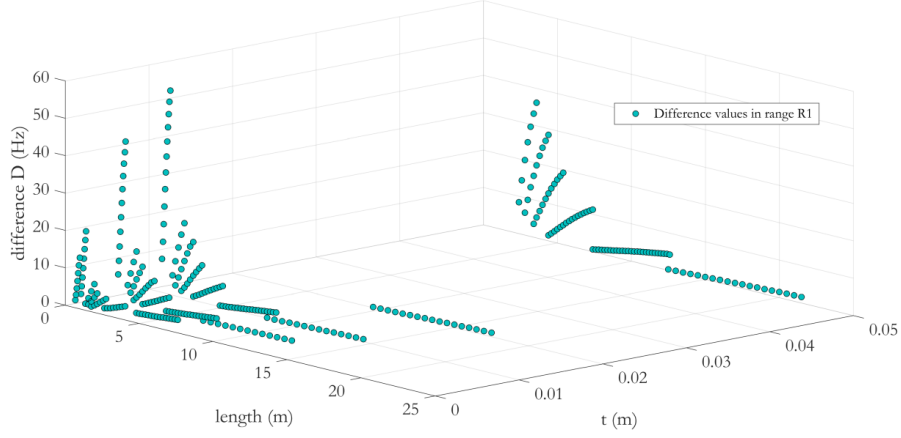


**Figure 5.3** Data points for term  $D$  that belong in region  $R_1$

Starting from the difference  $D$ , it was chosen to be multiplied by a term  $q$ ,

$$q = \sqrt{\frac{\rho v}{Ek^2}} \quad (5.4)$$

resulting to the dimensionless difference value,

$$D_0 = Dq \quad (5.5)$$

This was done on the basis of transitioning from Hz units, to a dimensionless quantity, and trying to also include important parameters other than the curvature, that are characterising the shell structures of interest, despite being constant in the current study. For the rest of the axes, the dimensionless quantities  $k\ell$  &  $kt$ , are introduced once again. Using the dimensionless quantities  $k\ell$ ,  $kt$  and  $D_0$ , instead of  $\ell$ ,  $t$  and  $D$ , respectively, leads to Figure 5.4. Clearly, it is managed to align all the points, but, still, their course along  $k\ell$  axis is displaying a concavity. It is not to be forgotten, that the outcome of this case study should not be too complex in favour of the convenience an engineer should feel using this formula. Therefore, this course that the points are showing, is not sufficient just yet, as it would require a more complex equation to describe them.

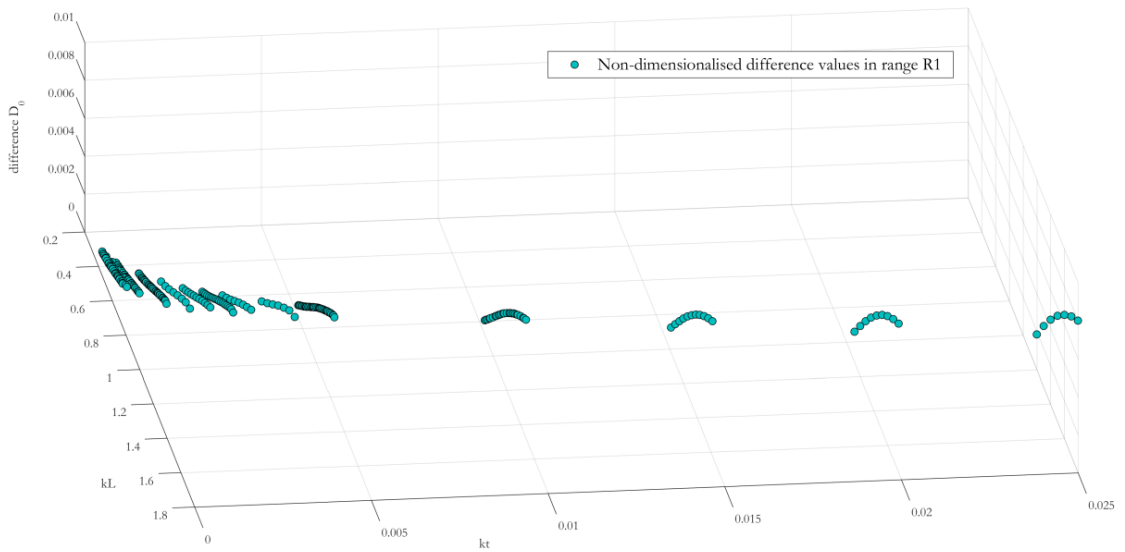


**Figure 5.4** Data points for term  $D$  in region  $R_1$ , plotted in dimensionless quantities

Having found the dimensionless quantities to work with, a proper scale should be discovered, so that this concavity can be reduced. For this purpose, the use of the exponential function is deployed. Data are being plotted again in Figure 5.5, with the help of the exponents of the discovered quantities. Their course can now be expressed by the equation of a flat linear surface that fits very accurately to them. This surface represents an estimation of the difference occurring between the ANSYS frequency and the base formula frequency, depending on length, thickness and curvature of the investigated panel. Consequently, the fitted surface relates to the searched term  $C$ , as it will be further demonstrated later

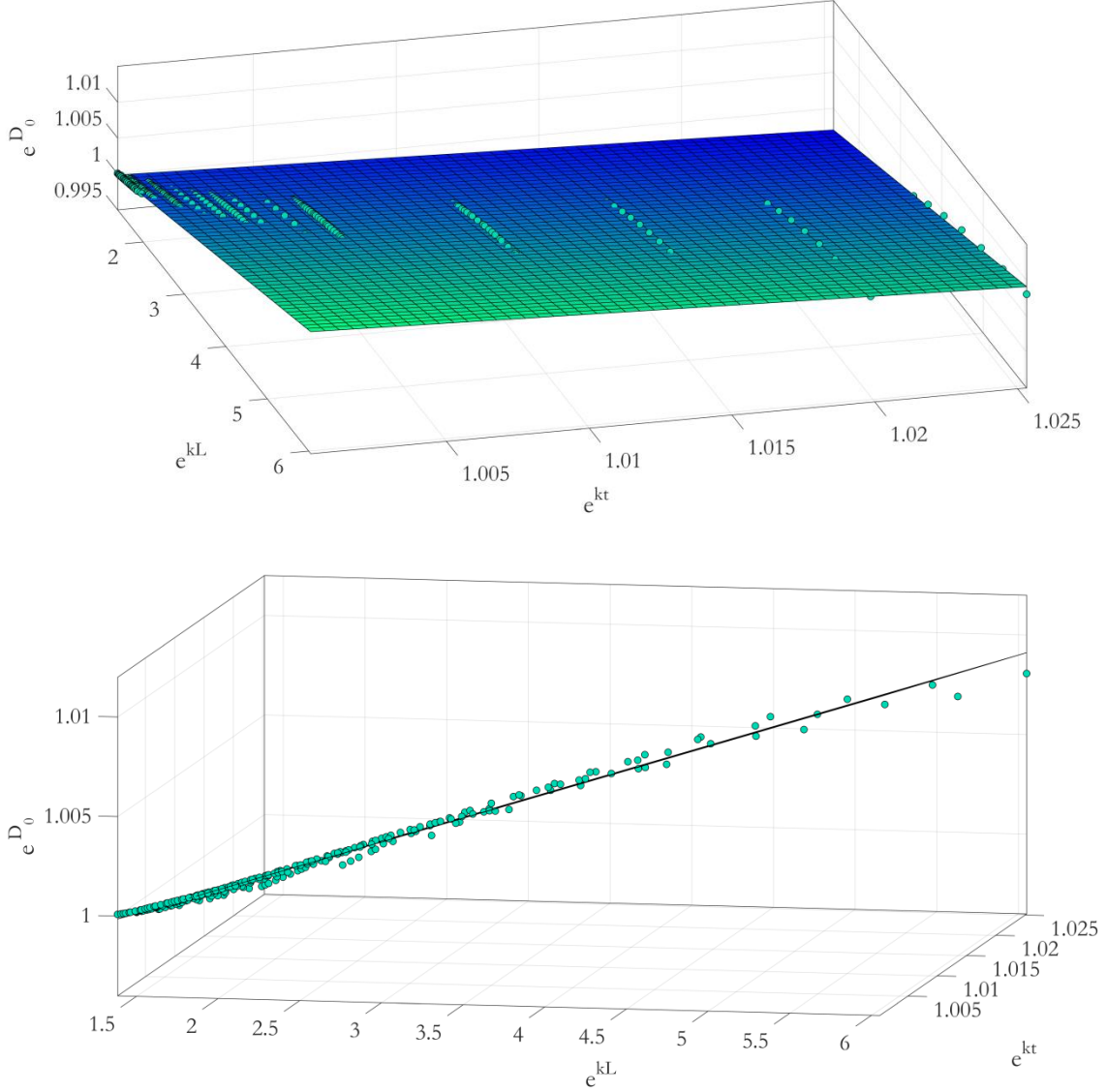


**Figure 5.5** Surface fit in region  $R_1$ , displayed from different perspectives

The equation of this surface is given by:

$$b_1 = e^{\overline{D_0}} = 1.1117 + 0.0026e^{k\ell} - 0.1154e^{kt} \quad (5.6)$$

where  $\overline{D_0}$  represents the approximated dimensionless difference. The homogeneity and the convenient values of the coefficients of this equation are mainly the reason why an exponential term was introduced to all the variables. An exponential term for the quantity  $k\ell$ , would be enough in the particular case, as the goal was to decrease the concavity, which appears along this axis.

### 5.3 Phase 2

Moving forward, the second part of the difference curves will be analysed. As it was previously distinguished, this part consists of the remaining of the difference values, located beyond the first peak. Derived in section 5.2, the expression that predict these peaks, already exists. Using eq. (5.3) and considering only the data points inside the limit  $k\ell \leq 2.0$ , the region  $R_2$  is defined. In the same manner previously, all the  $D$  values are plotted for this region in Figure 5.6.

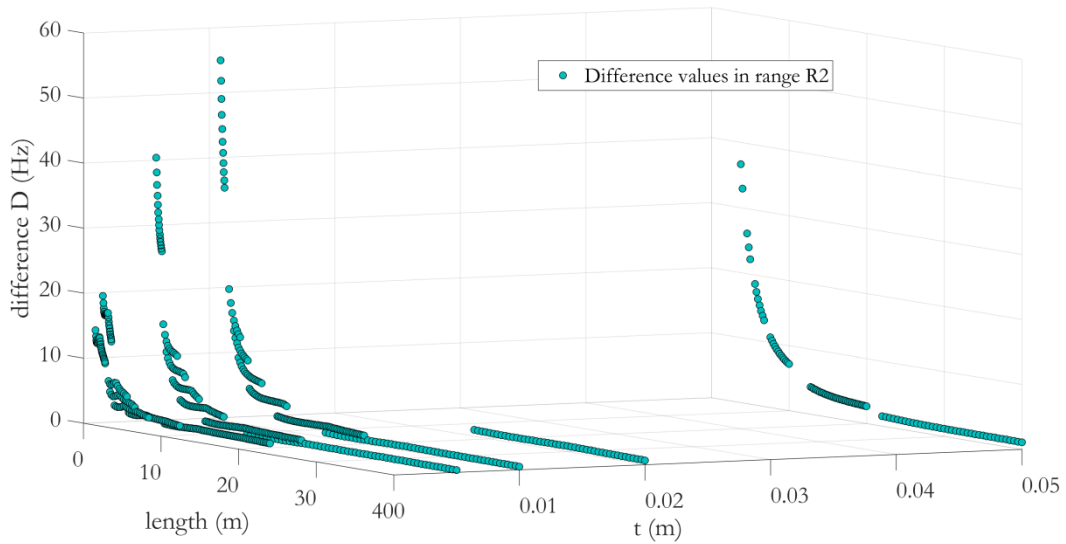


**Figure 5.6** Data points for term  $D$  in region  $R_2$

The approach, as well as the dimensionless quantities used, remain the same. Using the dimensionless quantities  $k\ell$ ,  $kt$  and  $D_0$ , provided by eq. (5.5), in place of the respective  $\ell$ ,  $t$  and  $D$ , leads to Figure 5.7. This is obviously a far more difficult pattern to be described when compared to the Figure 5.4, shown in the previous section. This was expected, though, due to the observations made in Chapter 4, where it was noticed that the inclined parts were demonstrating the advantage of being almost aligned, in contrast to the current examined part.

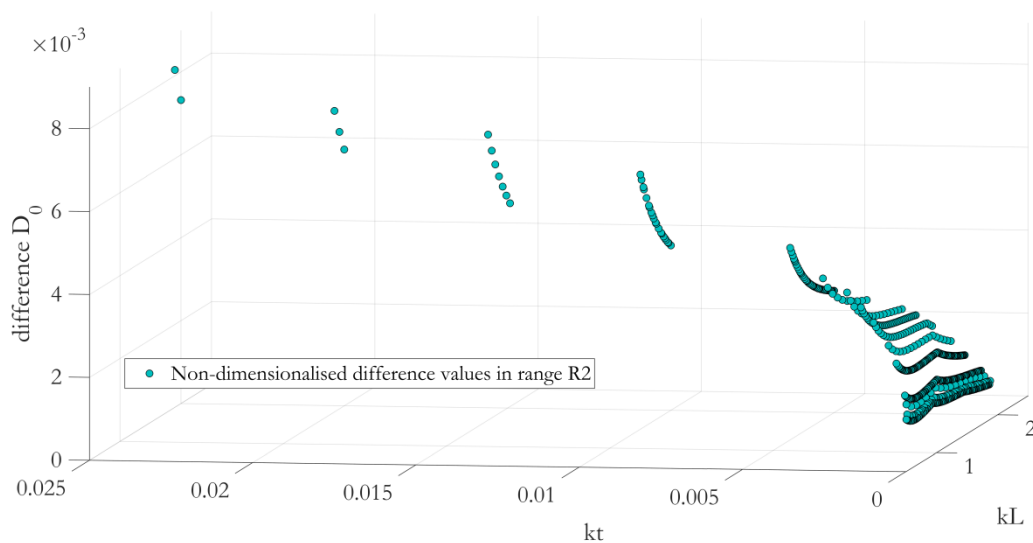


**Figure 5.7** Data points for term  $D$  plotted in a dimensionless space

Nevertheless, it has been remarked for all the remaining parts analysed here, that they are shifting either upwards and to the left or upwards and to the right, with the increase of curvature and thickness, respectively. This, reveals a close relation between  $k, t$  and  $D$ . Along with the distribution of the data points in Figure 5.7, the conclusion that these tendencies should be normalized in a different way than before came up. A smoother transition between the various cases is wanted here. This was achieved by modifying the axes  $kt$  and  $D_0$  in a similar way using natural logarithms, while axis  $k\ell$  was treated in the opposite way, with the help of the exponential term. As shown in Figure 5.8, the discrepancies were limited enough, so that a flat linear surface can once again be fitted sufficiently to all the data points.

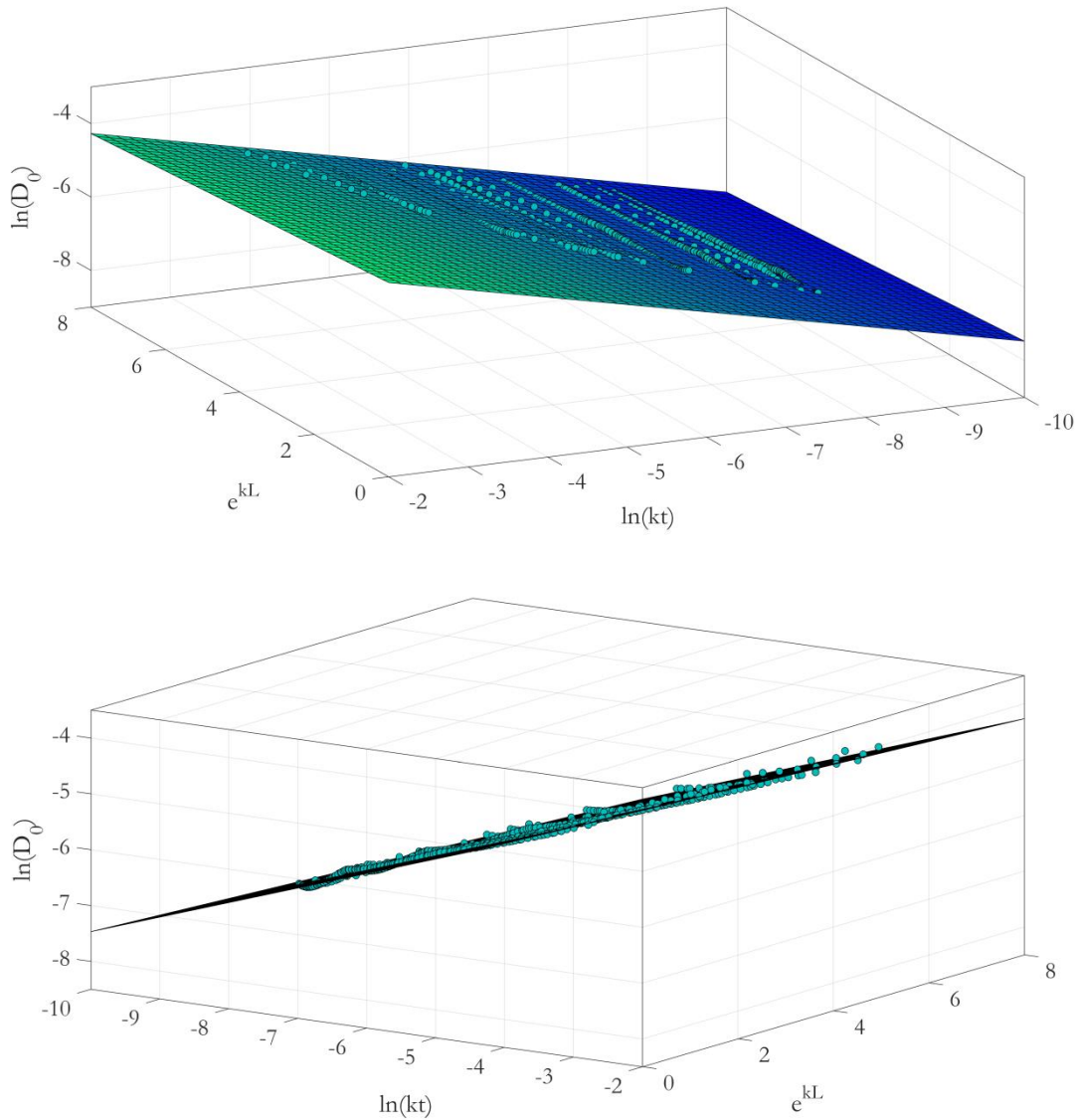


**Figure 5.8** Surface fit in region R<sub>2</sub>, displayed from different perspectives

This surface is described by the equation:

$$b_2 = \ln(\overline{D_0}) = -2.7656 - 0.0706e^{k\ell} + 0.4702 \ln(kt) \quad (5.7)$$

The above expression can be also interpreted as the value  $C$  that needs to be added in eq. (5.1) after properly transferring in the dimensions space, to return in Hz units. Conveniently, eq. (5.7) is quite similar to eq. (5.6), despite the various abnormalities this second part of the analysis was containing.

## 5.4 Derived formula

The equations derived previously in this Chapter, are combined herein to extract the final formula required. Regardless the regions mentioned, the starting point is common:

$$f = \sqrt{\frac{\pi^2 E t^2}{12(1 - \nu^2)\rho \ell^4}} + C$$

Term  $C$  is dependent on the region the investigated panel belongs. For a given combination of curvature and thickness, there is a region,  $R_0$ , inside which, the base formula is still applicable. If the shell structure of interest has length smaller than a certain value, term  $C$  is zero, and the prediction can be made by the base formula alone. The limit value for the length arises from eq. (5.2), and can be expressed as

$$k\ell < 3.0725(kt)^{0.2726}$$

If the above condition is not fulfilled, there are two other regions the shell could belong,  $R_1$  &  $R_2$ . Region  $R_1$  is defined by the boundaries

$$3.0725(kt)^{0.2726} \leq k\ell \leq 4.379(kt)^{0.2329} \quad (5.8)$$

where the right part came up due to eq. (5.3). For this case, Term  $C$ , can be obtained from eq. (5.6), recapped also here for convenience:

$$b_1 = e^{\overline{D}_0} = 1.1117 + 0.0026e^{k\ell} - 0.1154e^{kt} \quad (5.6)$$

This equation returns the exponential value of the approximated dimensionless difference,  $\overline{D}_0$ . For finding the estimated difference,  $\overline{D}$ , and return to Hz units, analogously to eq. (5.5), applies:

$$\overline{D} = \frac{\overline{D}_0}{q} \quad (5.9)$$

where

$$q = \sqrt{\frac{\rho v}{Ek^2}} \quad (5.4)$$

Term  $C$  must cover the difference between the base formula and the ANSYS frequency and should also be expressed in Hz units. Therefore,  $C = \overline{D}$  is wanted. For this purpose, taking the natural logarithm of  $b_1$ , and dividing it by  $q$ , leads to:

$$\frac{\ln b_1}{q} = \frac{\overline{D}_0}{q} = \overline{D} \xrightarrow{\text{eq.(5.4)}} C = \ln b_1 \sqrt{\frac{Ek^2}{\rho v}} \quad (5.10)$$

Proceeding to the next and last region,  $R_2$ , the boundaries found in a previous segment are shown here:

$$4.379(kt)^{0.2329} < k\ell \leq 2.0$$

Following the same approach as before, term  $C$  will result from the proper modification of eq. (5.7):

$$b_2 = \ln(\overline{D}_0) = -2.7656 - 0.0706e^{k\ell} + 0.4702 \ln(kt) \quad (5.7)$$

This time, the exponential function is deployed for transposing  $b_2$ , while dividing it once again by term  $q$ . Thus, in this region, term  $C$  is provided by:

$$\frac{e^{b_2}}{q} = \frac{\bar{D}_0}{q} = \bar{D} \xrightarrow{\text{eq.(5.4)}} C = e^{b_2} \sqrt{\frac{Ek^2}{\rho v}} \quad (5.11)$$

Summarising the above limits and all  $C$  terms for the different regions, into a more appealing and collective manner, results to the final formula developed:

$$f = \sqrt{\frac{\pi^2 Et^2}{12(1-v^2)\rho\ell^4}} + a \sqrt{\frac{Ek^2}{\rho v}} \quad (5.12)$$

where

$$a = \begin{cases} 0, & 3.0725(kt)^{0.2726} > k\ell \\ \ln b_1, & 3.0725(kt)^{0.2726} < k\ell < 4.379(kt)^{0.2329} \\ e^{b_2}, & 4.379(kt)^{0.2329} < k\ell \end{cases} \quad (5.13)$$

and

$$\begin{cases} b_1 = 1.1679 + 0.0028e^{k\ell} - 0.1719e^{kt} \\ b_2 = -2.7953 - 0.0686e^{k\ell} + 0.4674 \ln(kt) \end{cases} \quad (5.14)$$

The reader should take notice that the above expressions are very sensitive to changes in decimal values and it is not advised to round up any of the values.

## 6 EVALUATION OF THE RESULTS & VALIDITY LIMITS

### 6.1 Visualisation of the result

In an attempt to visualise the outcome of the approximation made with the new formula, the case for a panel with  $k=0.1 \text{ m}^{-1}$  and  $t=0.005 \text{ m}$ , originally examined in section 4.2, is replotted here in Figure 6.1. Focusing once again on the area the curve of ANSYS frequency was starting to separate from the one of the base formula, the difference in the agreement between region  $R_1$  and  $R_2$  is clearly noticeable. Besides, this was predicted already based on the observations in Chapter 4. Nevertheless, the peaks could not be approximated better without a more complicated term coming in, or perhaps without splitting the introduced regions in more parts.

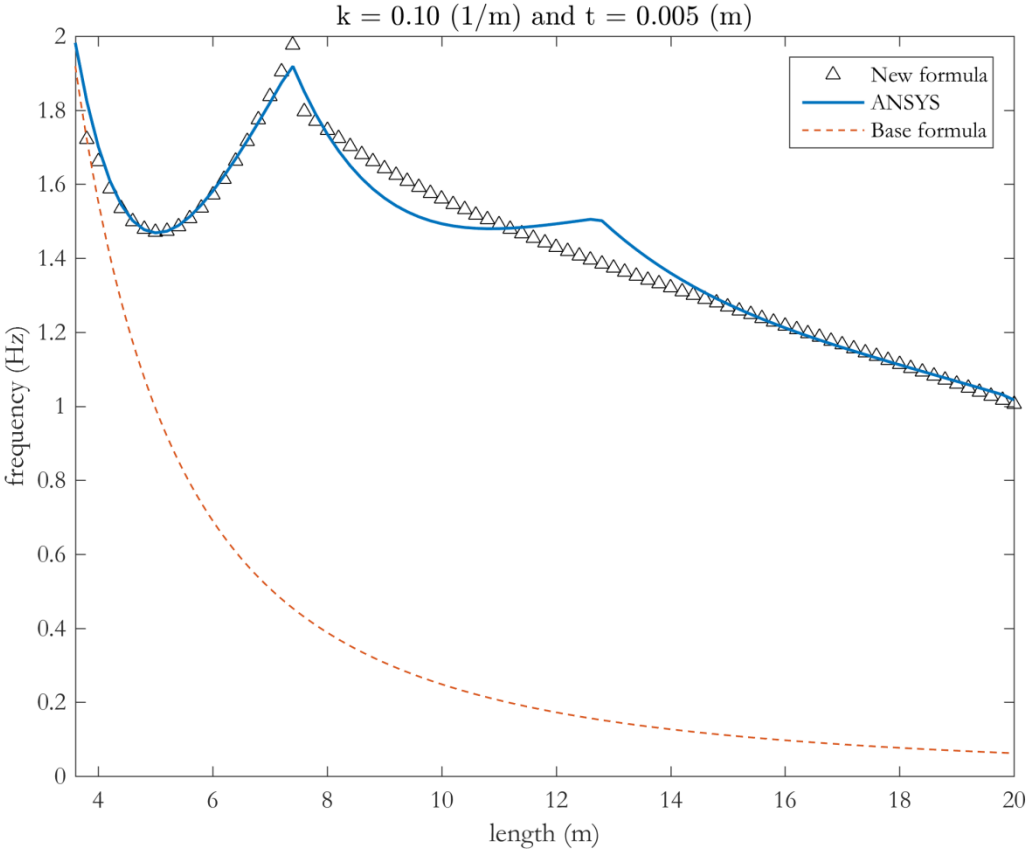


**Figure 6.1** Accordance of derived formula with ANSYS data, for Case 2 with  $t=0.005\text{m}$  (scaled)

Proceeding, the new formula is examined in respect to the curvature variation. In section 4.5 and especially in Figure 4.12, a significant relocation was observed in between curves, due to  $k$  values. It was also seen that base formula was resulting to only one curve. All the fitted curves for each of the seven cases of the curvatures, provided by the appropriate introduced terms depending on the distinguished regions, are displayed in Figure 6.2.

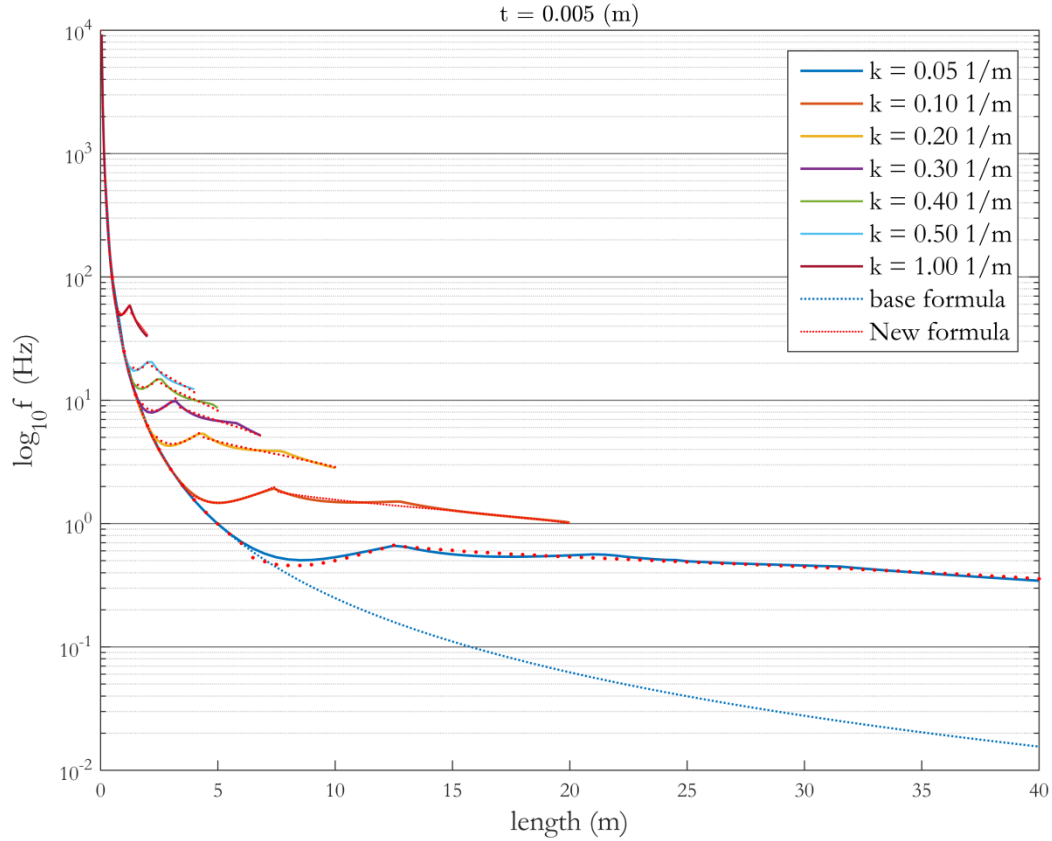


**Figure 6.2** Accordance of the derived formula with ANSYS data, for all cases with  $t=0.005\text{m}$

## 6.2 Error assessment

The approach followed to evaluate the formula derived in the previous Chapter, is to apply it for all the models created when the data were collected and investigate the new margin of error that arises. The process was automated by a MATLAB script which inputs the various values of length, curvature and thickness to the formula, determines the region the shell belongs, as well as the value of  $\alpha$ , and returns the prediction. Afterwards, the script compares the estimation to the ANSYS frequency and all the error values that are above the desirable condition set, are stored, indicating simultaneously the combination  $k\ell$  and  $kt$  for which they occur.

Previous studies were aiming to achieve a margin of error of 20%. Setting this condition initially, the developed script returned a total of 6 cases that exceeded this limit. The number of models checked were 1396. Investigating the properties of those cases, it is noticed that they are all referring to a model that belong in the region  $R_0$ , where no corrections were made to the base formula. However, trying to visualise those shells, it can be seen that they are not corresponding to reality, as they have minimal lateral dimensions when comparing to their thickness. This was also discussed in section 4.4 & 4.5 and will be avoided with the boundaries to be set for the validity of the formula. Therefore, the aforesaid extreme cases are not a problem and the formula works perfectly for the whole range examined.

Trying to identify the quality of the resulted formula, the error values that are greater than 15% are now searched. This, results to 3 adding cases other than the previously derived. Those errors are just above 15% and emerge for a model which is characterized by either  $r/t = 4000$ , or  $r/t = 40$ , where  $r$  is the radius of the curvature. Obviously, these values are poles apart and they are basically constituting the boundaries for a shell to be considered as thin, and also the boundaries for the data acquisition of this

study. The appearance of those errors, underlies that, an attempt to enclose the disparities in the behaviour for such different types of panels might cause a reduction in the accuracy of the formula.

Next, the condition for an even lower margin of error was set. The shells appearing an error more than 10% were found, amounting to 37 (including the above 9). Those 28 models were investigated further to find if there was a relation between them or were randomly distributed. Indeed, all the cases showed something in common. As before, these shells were correlating to each other with the help of the quantity  $kt$ , here expressed as  $r/t$ . The correspondence between all the occurred errors is that they appear for curved panels with ratios  $r/t \leq 100$ , or  $r/t \geq 3333.33$ .

### 6.3 Validity limits of the derived formula

After examining the errors, two options are arising regarding the application limits of the new formula: the one is to sacrifice the accuracy in pursuing of wider limits, while the other is to establish a narrower spectrum of validity and thus, assure higher quality estimations. It is chosen to adopt the second viewpoint. Besides, the restrains applied in order to achieve this, are not considered to be of major significance.

Beginning from the quantity,  $kt$ , and taking into a consideration the instances of error seen to transcend the 10% mark, led to the following limit:

$$\frac{1}{100} > kt > \frac{1}{3300} \quad (6.1)$$

Concerning the length, an upper limit already exists as arises from the data acquisition. A lower limit needs to be introduced, due to the abnormalities shown in very small dimensions and the limited research in this region. As mentioned in section 4.5, before coming to any conclusion about whether the error exceeds the desirable margin in this area, the influence of curvature should be looked upon. It was noted that, it was not sufficient to explain the behaviour of the natural frequency based only on the assumptions made by Blevins. For this reason, the cases presenting these errors are further investigated here. Due to their limited number, it is easy to come up with some conclusions regarding their correlation. All the values, except one, have something in common in groups. That is, the values themselves. They can be assembled as one group that has values around -11% and another that has values of about -28%. These values are plotted in Figure 6.3 to distinguish their correlation. Evidently, the points plotted are following a rather weak quadratic trend, which could potentially be described sufficiently with a simple linear equation.

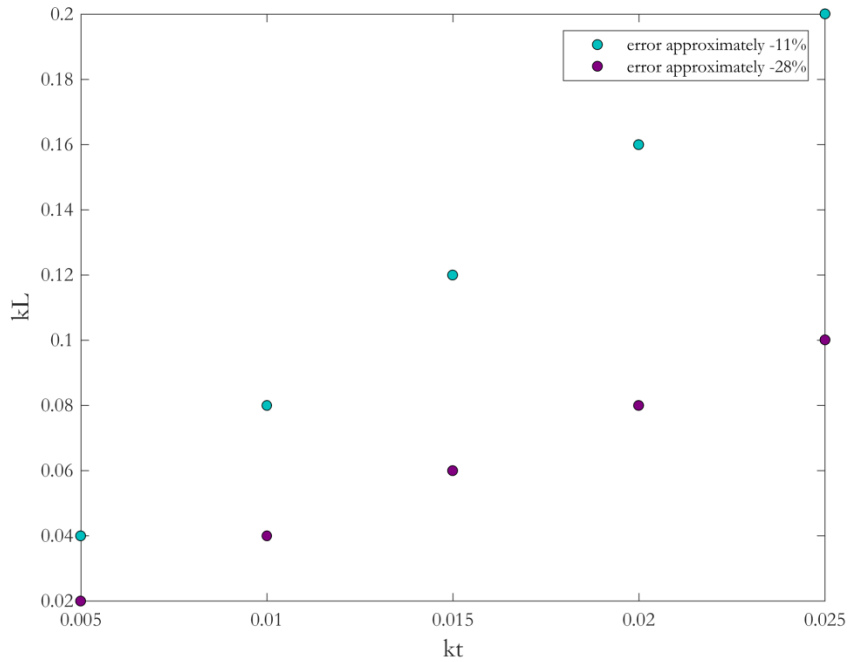


**Figure 6.3** Data points for minimal lengths in region  $R_0$  that exceed the 10% error mark

It has to be remarked that, in Figure 6.3, there are also values of  $kt$  displayed, that fall out of the defined range in respect to the expression (6.1). Neglecting the points that belong to this region, more data need to be obtained in order to find a relation as a restriction to the accuracy boundaries of the new formula. The data were collected, on the basis of resulting to an error close to the 10% value set as a goal herein. Acquiring the natural frequency of some more models and comparing it with the base formula, a homogenous set of points that had values of almost -10%, was possessed. Similarly to above, where all the examined data had common values of error in groups, an aligned trend is also expected. Given the fact that the range of  $kt$  is narrower, an even more reduced concave shape is expected. Indeed, in Figure 6.4, the correlation between the points is utterly perfect and conveniently, easily described.

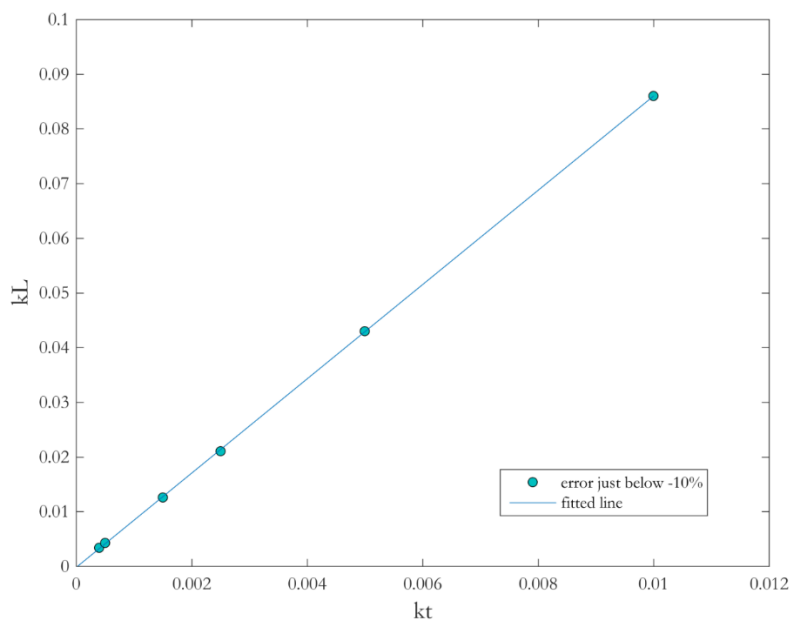


**Figure 6.4** Alignment of data points in region  $R_0$  with error about -10%

The best possible fitted line is given by,

$$k\ell = 8.6194(kt) - 2.1 \cdot 10^{-4} \quad (6.2)$$

which for simplicity, without significant accuracy loss, and being also on the safe side, can be written as

$$k\ell = 8.62(kt) \quad (6.3)$$

where  $k\ell$  is the limit value, above which, the formula of the study is applicable.

Altogether, the validity limits of the derived formula for the prediction of the natural frequency of the anticlastic shells of study, within a margin of error of 10%, are constituted as stated below:

$$\frac{1}{100} > kt > \frac{1}{3300} \quad \text{and} \quad 8.62(kt) \leq k\ell \leq 2.0 \quad (6.4)$$

## 7 CONCLUSIONS AND RECOMMENDATIONS

In the current study, a total of 1396 finite-element models were generated and analysed, to investigate the influence of various parameters on anticlastic curved panels made of steel. The focus of the study was to examine the effect of length, thickness and curvature, on the lowest natural frequency of simply supported thin shell structures and to, finally, derive a formula that would accurately estimate its values.

The formula developed is

$$f = \sqrt{\frac{\pi^2 E t^2}{12(1-\nu^2)\rho \ell^4}} + a \sqrt{\frac{E k^2}{\rho \nu}} \quad (5.12)$$

where

$$a = \begin{cases} 0, & 3.0725(kt)^{0.2726} > k\ell \\ \ln b_1, & 3.0725(kt)^{0.2726} < k\ell < 4.379(kt)^{0.2329} \\ e^{b_2}, & 4.379(kt)^{0.2329} < k\ell \end{cases} \quad (5.13)$$

and

$$\begin{cases} b_1 = 1.1679 + 0.0028e^{k\ell} - 0.1719e^{kt} \\ b_2 = -2.7953 - 0.0686e^{k\ell} + 0.4674 \ln(kt) \end{cases} \quad (5.14)$$

It was shown that it is impossible to approximate perfectly all the tendencies of the lowest natural frequency with one universal formula, due to the irregular shape occurring when transitioning between the dominant vibration mode shapes. Thus, the formulation carried out in parts. The study leaves promises for a perfect correspondence between the actual frequency and the estimation by attempting to divide the problem in more parts. This can be further researched if better accuracy is sought.

Important to notice is that curvature was found to not affect significantly the natural frequency in small lengths, while in minimal dimensions appeared to be an inverse relation to what seen in later lengths. This was discussed in section 4.5 and is worth mentioned to be further investigated.

The limits of the formula were established on the basis of the preference the new formula to return estimations within a margin of error 10%. The validity range of the formula is decided by,

$$\frac{1}{100} > kt > \frac{1}{3300} \quad \text{and} \quad 8.62(kt) \leq k\ell \leq 2.0 \quad (6.4)$$

These conditions can be modified according to the accuracy desired. It is believed that the formula is also valid within a margin of error of 10%, for a wider range than the one constrained by  $k\ell \leq 2.0$ . This would expand even more the applicability of the formula and is advised to be looked upon.

Despite the wide range achieved to be approximated, this formula is valid only for shells that satisfy a series of assumptions: the curved panel has no twist, length and curvatures along both the axis have the same absolute values, is simply supported, and Young's modulus, Poisson's ratio and density remain constant in all the cases examined. Therefore, a further step, could be to investigate the influence of those rest parameters.

Ultimately, it is believed that this formula can lead to the development of a shell buckling model, which is of dominant significance in designing thin shells. For specific shapes, such as cylinders and spheres, much literature is available. The current study, could prove to be a valuable asset to this literature.

## REFERENCES

- [1] Blaauwendraad J.& Hoefakker J.H., *Structural Shell Analysis: Understanding and Application (Vol. 200)*, Dordrecht: Springer, 2014.
- [2] Blevins R.D., *Formulas for natural frequency and mode shape*, New York: Van Nostrand Reinhold Company, 1979.
- [3] van Dijk R., *Eigenfrequenties van schalen; Uitbreiding van de ontwerpformule*, TU Delft, 2014.
- [4] Greijmans M. L., *Eigenfrequenties van schalen: Uitbreiding van de ontwerpformule*, TU Delft, 2016.
- [5] Hoogenboom, P.C.J., *CIE4143 Shell Analysis, Theory and Application*, lecture notes
- [6] Metselaar, L., *Een ontwerpformule voor de laagste eigenfrequentie van gekromde panelen*, TU Delft, 2013.
- [7] Moerbeek C.M., *De invloed van kromming op de eigenfrequentie van oppervlaktes*, TU Delft, 2012.
- [8] Noortman F.J., *Ontwerpformule voor de eigenfrequentie van schalen*, TU Delft, 2015.
- [9] Paasman Y., *Eigenfrequentie van gekromde panelen; Totstandkoming van een ingenieursformule*, TU Delft, 2016
- [10] Peerdeman B., *Analysis of Thin Concrete Shells Revisited: Opportunities due to Innovations in Materials and Analysis Methods*, TU Delft, 2008
- [11] Scheltema A., *Eigenfrequenties, Dubbele Krommingen & Twist*, TU Delft, 2013.
- [12] Sluijs J., *Eigenfrequentie van gekromde panelen: Uitbreiding van de ontwerpformule voor zadelvormige panelen*, TU Delft, 2017
- [13] Timoshenko S.P. & Woinowsky-Krieger S., *Theory of Plates and Shells; International Student Edition (Second Edition)*, New York, McGraw-Hill Book Company, 1959
- [14] Webster J.J., *Free vibrations of rectangular curved panels*, International Journal of Mechanical Sciences, 10(7), 571-582., 1968

## APPENDIX A

This appendix contains the script used for generating and analysing the finite-element models in ANSYS. It is written in APDL and is also suitable for shells with twist and unequal lengths and curvatures. The fields ‘(...input...)’ are not part of the scripting language. They simply represent the values given to the variables for each model.

```

!----- input data -----
l = (...input...)! (m)           set value for length
lx = l           ! (m)           length of shell panel in the x-direction
ly = l           ! (m)           length of shell panel in the y-direction
t = (...input...)! (m)           set value for thickness
k = (...input...)! (1/m)         set value for curvature
kxx = -0.1       ! (1/m)         curvature along the xx axis
kyy = 0.1        ! (1/m)         curvature along the yy axis
kxy = 0.00       ! (1/m)         twisting
E = 2.1e11       ! (N/m^2)       Young's elastic modulus
nu = 0.33        ! (-)           Poisson's ratio
rho = 7850       ! (kg/m^3)      mass density
!----- end -----

/PREP7                               ! Enters the model creation pre-processor.

!----- define material, element type and thickness -----
/PREP7
MPTEMP,,,,,,,,                       ! isotropic material
MPTEMP,1,0                             !      »      »
MPDATA,EX,1,,E                          !      »      »
MPDATA,PRXY,1,,nu                       !      »      »
MPDATA,DENS,1,,rho                      !      »      »
ET,1,SHELL181                           ! 4-node structural shell
R,1,t,t,t,t, , ,                       ! thickness as of above
!----- end -----

!----- generate nodes -----
*DO,i,0,n
  *DO,j,0,n
    x=lx/n*i-lx/2
    y=ly/n*j-ly/2
    z1=0.5*x*x*kxx
    z2=x*y*kxy
    z3=0.5*y*y*kyy
    z=z1+z2+z3
    N,,x,y,z,,
  *ENDDO
*ENDDO
!----- end -----

!----- generate elements -----
*DO,i,1,n
  *DO,j,1,n
    k=i+(j-1)*(n+1)
    E,k,k+1,k+n+2,k+n+1
  *ENDDO
*ENDDO
!----- end -----

!----- rotate the CS of all nodes -----
*DO,i,1,(n+1)*(n+1)
  xx=1
  xy=0
  xz=NX(i)*kxx+NY(i)*kxy
  lx=SQRT(1+xz*xz)
  zx=-NX(i)*kxx-NY(i)*kxy
  zy=-NX(i)*kxy-NY(i)*kyy
  zz=1
  lz=SQRT(zx*zx+zy*zy+1)
  NANG,i,xx/lx,xy/lx,xz/lx,,,zx/lz,zy/lz,zz/lz
*ENDDO
!----- end -----

```

```

!----- rotate the CS of the nodes in the edge x = - lx/2 -----
*DO,i,2,n
  yx=0
  yy=1
  yz=NX(i)*kxy+NY(i)*kyy
  ly=SQRT(1+yz*yz)
  zx=-NX(i)*kxx-NY(i)*kxy
  zy=-NX(i)*kxy-NY(i)*kyy
  zz=1
  lz=SQRT(zx*zx+zy*zy+1)
  NANG,i,,,,yx/ly,yy/ly,yz/ly,zx/lz,zy/lz,zz/lz
*ENDDO
!----- end -----

!----- rotate the CS of the nodes in the edge x = lx/2 -----
*DO,i,2,n
  j=n*(n+1)+1
  yx=0
  yy=1
  yz=NX(j)*kxy+NY(j)*kyy
  ly=SQRT(1+yz*yz)
  zx=-NX(j)*kxx-NY(j)*kxy
  zy=-NX(j)*kxy-NY(j)*kyy
  zz=1
  lz=SQRT(zx*zx+zy*zy+1)
  NANG,j,,,,yx/ly,yy/ly,yz/ly,zx/lz,zy/lz,zz/lz
*ENDDO
!----- end -----

!----- BC: no displacement perpendicular to the plane -----
*DO,i,1,n
  j=i
  D,j,UZ,0
  j=i*(n+1)
  D,j,UZ,0
  j=i+n*(n+1)+1
  D,j,UZ,0
  j=i*(n+1)+1
  D,j,UZ,0
*ENDDO
!----- end -----

!----- BC: no displacement in the directions of the edges -----
*DO,i,1,n+1
  D,i,UY,0
*ENDDO
*DO,i,n*(n+1)+1,(n+1)*(n+1)
  D,i,UY,0
*ENDDO
*DO,i,1,n*(n+1)+1,n+1
  D,i,UX,0
*ENDDO
*DO,i,n+1,(n+1)*(n+1),n+1
  D,i,UX,0
*ENDDO
!----- end -----

FINISH                                ! Exits normally from the pre-processor.

/SOLU                                  ! Enters the solution processor.

ANTYPE, 0                              ! Specifies the analysis type as static.

/STATUS,SOLU                           ! Provides a solution status summary.

SOLVE                                  ! Starts the solution.

FINISH                                  ! Exits normally from the solution
! processor.

/SOLU                                  ! Enters the solution processor.

ANTYPE,MODAL                           ! Specifies the analysis type as modal.

MODOPT, LANB, 10,,,                   ! Block Lanczos, 10 modes to extract.

MXPAND,10                              ! Expand & write 10 modes to the results
! file.

```

```

PSTRES,ON          ! Prestress effects are calculated.

SOLVE             ! Starts the solution.

FINISH           ! Exits normally from the solution
                ! processor.

/POST1           ! Enters the database results
                ! postprocessor.

/SHOW,WIN32C     ! Specifies the device for graphics
                ! displays.

SET,FIRST        ! Read the first data set from the results
                ! file.

/PLOPTS,INFO,3   ! Graphics : switch to Multi-legend mode.

/CONTOUR,ALL,18  ! Specifies the uniform contour values on
                ! stress displays as 18 in ALL windows.

/PNUM,MAT,1      ! Turns ON numbering/coloring for MAT
                ! label.

/NUMBER,1        ! Color the numbered items. Do not show
                ! the numbers.

/REPLOT,RESIZE   ! Automatically reissues the last display
                ! command for convenience.

PLNSOL,U,Z       ! Displays results as continuous contours
                ! for Z-axis structural displacement.

SET,,,,,,,,1     ! Read data set number 1.

```

## APPENDIX B

This appendix encloses the script composed for deriving the formula.

```
%import data f and L
%***ATTENTION!*** Use "numeric matrix" format, replacing the...
%...unimportable cells with '0' value!

clearvars -except f L

%-----BLOCK 1_DEFINE MATERIAL PROPERTIES AND VARIABLES-----
E = 2.1e11;
rho = 7850;
v = 0.33;

t = [0.005 0.01 0.02 0.05...
     0.0025 0.005 0.010 0.050...
     0.0015 0.005 0.010 0.050...
     0.001 0.005 0.010 0.050...
     0.001 0.005 0.010 0.050...
     0.001 0.005 0.010 0.050...
     0.0005 0.001 0.005 0.010];

k = [0.05 0.1 0.2 0.3 0.4 0.5 1.00];
%-----end BLOCK 2-----

%----- BLOCK 2_BASE FORMULA vs ANSYS FREQUENCY-----
%Preallocate memory
fb = zeros(size(f,1),size(f,2)); diff = fb; error = fb; C = fb;
fnew = fb; diffnew = fb; errornew = fb;

tpc = size(f,2)/size(L,2); %thicknesses per case

ind = 1;
for j = 1:size(f,2)
    for i = 1:nnz(L(:,ind))
        % frequency estimation of the base formula:
        fb(i,j) = sqrt((pi^2*E*t(j).^2)/(12*(1-v^2)*rho*L(i,ind).^4));
        % difference between frequency from ANSYS and the base formula:
        diff(i,j) = f(i,j) - fb(i,j);
        %margin of error ('%' value) between frequency from ANSYS and the
        base formula:
        error(i,j) = 100*diff(i,j)/f(i,j);
    end
    if (j/tpc == ind) %condition to identify the correct corresponding...
        ind = ind + 1; %...values of 'k' and 'L' to be used in each loop
    end
end
%-----end BLOCK 2-----

%-----BLOCK 3_DEFINE REGIONS-----
%preallocate memory
erL = zeros(1,size(f,2)); erkt = erL; erkL = erL; errorstart = erL;
spo = zeros(1,size(f,2)); kLspo = spo; ktspo = spo;
difftemp = zeros(size(f,1),size(f,2)); kLtemp = difftemp;

%-----R1 lower limit:error over 5-----
%{
%find a relation between the curvature, length and thickness that...
%...describes the point where the margin of error becomes over 5 percent:
```

```

%}
ind=1;
for j = 1:size(f,2)
    logic = 0; %logical index
    for i = 1:size(f,1)
        if (error(i,j) > 5) && (logic == 0) %find only the first length...
            logic = 1; %...value for which error>5%
            erL(j) = L(i,ind); %store this length
            erkL(j) = k(ind).*erL(j); %introduce dim/less quantity k*L
            erkt(j) = k(ind).*t(j); %introduce dim/less quantity k*t
            errorstart(j) = i; %row in which error exceeds 5%
        end
    end
    if (j/tpc == ind)
        ind = ind + 1;
    end
end
%{
%row vector 'erkL' contains the value 'kL' corresponding to each...
%... respective 'kt' combination, for which the error is greater than...
%...5 percent for the first time.
%The relation between the above 'kL' & 'kt' values can be described by...
%... a power model "y=ax^b" where x->erkt & y->erkL:
%}
[errorover5,ergof] = fit(erkt',erkL','power1'); %find the function &...
%...goodness of the fit

coeferr = coeffvalues(errorover5)'; %store the coefficients of this...
%...function

clear erL erkt erkL logic
%-----end error over 5-----

%-----R1 upper limit:first peak-----
%{
%find a relation between the curvature, length and thickness that describes
the point where...
%...first peak of the difference between frequency from ANSYS and the
'base' formula occurs:
%}
ind=1;
for j = 1:size(f,2)
    [~,locsD] = findpeaks(diff(:,j)); %locate all the peaks
    temp(:,j) = locsD; %store their locations in a matrix
    spo(j) = temp(1,j); %keep only the location of 1st peak
    kLspo(j) = k(ind).*L(spo(j),ind); %introduce dim/less quantity k*L
    ktspo(j) = k(ind).*t(j); %introduce dim/less quantity k*t
    if (j/tpc == ind)
        ind = ind + 1;
    end
end
%{
%Row vector 'kLspo' contains the value 'kL' corresponding to each
respective...
%...'kt' combination, for which the first peak of the difference between
frequency...
%... from ANSYS and the 'base' formula occurs. The data can be described...
%...by a power model y=ax^b where x->ktspo & y->kLspo:
%}

```

```

[peak,peakgof] = fit(ktspo',kLspo','power1');    %find the function &...
                                                %...goodness of the fit
coefpeak = coeffvalues(peak)';                %store the coefficients of this...
                                                %...function

clear locsD temp
%-----end first peak-----

%-----BLOCK 4_FITTING SURFACES-----
%{
%find the surface that fits through the non-dimensionalized difference...
%...values, when plotted against the also dimensionless quantities...
%...'kL' & 'kt'. This is done in two parts:
%Part 1: Surface for a range of 'kL' falling inside R1 region...
%Part 2: Surface for a range of 'kL' beyond the upper limit of R1 and...
%...until the limit of 'kL<2.0'. This is defined as R2 region.
%}
%PART 1: inside R1
ind=1;
count = 0;
for j = 1:size(f,2)
    for i = 1:size(f,1)
        %define conditions and ignore the zero values earlier imported:
        if errorover5(k(ind).*t(j))/k(ind) < L(i,ind) && diff(i,j) ~= 0...
            && peak(k(ind).*t(j))/k(ind) > L(i,ind)
                %{
                %create vectors with the proper dim/less quantities...
                %...of difference, length and thickness that belong in the...
                %...above mentioned range. The expressions are such, so that...
                %...the fit surface can be described by a simple equation
                %}
                count = count + 1;
                diffbp(count) = exp(diff(i,j).*sqrt(rho*v/E)./k(ind));
                kLbp(count) = exp(L(i,ind).*k(ind));
                ktbp(count) = exp(k(ind).*t(j));
            end
        end
        if (j/tpc == ind)
            ind = ind + 1;
        end
    end
end
%{
%selecting the proper expressions for the difference,length and...
%...thickness values, results to a flat fitted surface which has a simpler
%...and shorter equation. Therefore,the relation of the variables is of...
%...the form: g(x,y) = a + b*x + c*y, where x->kLbp, y->ktbp, g->diffbp
%}
[sfbp,gofbp] = fit([kLbp',ktbp'],diffbp','poly11'); %find the function &...
                                                %the goodness of fit

coefbp = coeffvalues(sfbp)';                %store the coefficients of this function

%PART 2: inside R2
ind=1;
count = 0;
for j = 1:size(f,2)
    for i = 1:size(f,1)
        %define conditions and ignore the zero values earlier imported:
        if (peak(k(ind).*t(j))/k(ind) < L(i,ind)) ...
            && (diff(i,j) ~= 0)

```

```

        %{
        %create vectors with the proper non-dimensionalized...
        %...quantities of difference, length and thickness that...
        %...belong in the above mentioned range. The expressions are...
        %...such, so that the fit surface can be described by the...
        %...simplest possible equation
        %}
        count = count + 1;
        diffap(count) = log((diff(i,j)).*sqrt(rho*v/E)./k(ind));
        kLap(count) = exp(L(i,ind).*k(ind));
        ktap(count) = log(k(ind).*t(j));
    end
end
if (j/tpc == ind)
    ind = ind + 1;
end
end
%{
%selecting the proper expressions for the difference,length and...
%...thickness values, results to a flat fitted surface which has a...
%...simpler and shorter equation. Therefore,the relation of the...
%...variables, is of the form: g(x,y) = a + b*x + c*y, where x->kLap,...
%...y->ktap, g->diffap
%}
[sfap,gofap] = fit([kLap',ktap'],diffap','poly11'); %find the function...
                                                %...and the goodness of fit

coefap = coeffvalues(sfap)'; %store the coefficients of this function
%-----end BLOCK_4-----

%-----BLOCK_5 FORMULA DEVELOPMENT-----
ind = 1;
for j = 1:size(f,2)
    for i = 1:nnz(L(:,ind))
        %added term, which will cover the difference, introduced as 'C':
        if (errorover5(k(ind).*t(j))/k(ind) < L(i,ind))...
            && (peak(k(ind).*t(j))/k(ind) > L(i,ind))
            C(i,j)=log(sfbp(exp(k(ind).*L(i,ind)),exp(k(ind).*t(j))))./...
                sqrt(rho*v/E).*k(ind);
        elseif (peak(k(ind).*t(j))/k(ind) < L(i,ind))
            C(i,j)=exp(sfap(exp(k(ind).*L(i,ind)),log(k(ind).*t(j))))./...
                sqrt(rho*v/E).*k(ind);
        else
            C(i,j) = 0;
        end
        %new formula:
        fnew(i,j) .= sqrt((pi.^2*E*t(j).^2)/(12*(1-v^2)*rho*L(i,ind).^4))...
            + C(i,j);
        % difference between frequency from ANSYS and the new formula:
        diffnew(i,j) = f(i,j) - fnew(i,j);
        %margin of error between frequency from ANSYS and the new formula:
        errornew(i,j) = 100*diffnew(i,j)/f(i,j);
    end
end
if (j/tpc == ind)
    ind = ind + 1;
end
end
%-----BLOCK_5 FORMULA DEVELOPMENT-----

```

```

%-----BLOCK_5 ERROR ASSESSMENT-----
%find the number of occasions and the locations where error is greater than
'10%':
ind=1;
num = 1;
errorcheck(num,:) = {'value','column','row','kt','kL'};
for j = 1:size(f,2)
    for i = 1:size(f,1)
        if (errornew(i,j) > 10) || (errornew(i,j)) < -10
            num = num + 1;
            kttemp = k(ind).*t(j);
            kLtemp = k(ind).*L(i,ind);
            errorcheck(num,:) = {errornew(i,j),j,i,kttemp,kLtemp};
        end
    end
    if (j/tpc == ind)
        ind = ind + 1;
    end
end
clear ind i j kttemp kLtemp

```

## APPENDIX C

Table C1 Comparison of ANSYS and formula frequencies for Case 1.

L [m]	$k = 0,05 \text{ [m}^{-1}\text{]}$											
	$t = 0,005 \text{ [m]}$			$t = 0,010 \text{ [m]}$			$t = 0,020 \text{ [m]}$			$t = 0,050 \text{ [m]}$		
	$f_{\text{ANSYS}}$ [Hz]	$f_{\text{FORMULA}}$ [Hz]	ERROR [%]	$f_{\text{ANSYS}}$ [Hz]	$f_{\text{FORMULA}}$ [Hz]	ERROR [%]	$f_{\text{ANSYS}}$ [Hz]	$f_{\text{FORMULA}}$ [Hz]	ERROR [%]	$f_{\text{ANSYS}}$ [Hz]	$f_{\text{FORMULA}}$ [Hz]	ERROR [%]
0,5	99,158	99,380	-0,224	197,267	198,761	-0,757	389,308	397,522	-2,110	923,686	993,804	-7,591
1,0	24,819	24,845	-0,107	49,550	49,690	-0,283	98,576	99,380	-0,816	241,358	248,451	-2,939
1,5	11,024	11,042	-0,168	22,029	22,085	-0,253	43,932	44,169	-0,539	108,483	110,423	-1,788
2,0	6,193	6,211	-0,290	12,380	12,423	-0,340	24,717	24,845	-0,517	61,277	62,113	-1,364
2,5	3,958	3,975	-0,448	7,912	7,950	-0,490	15,804	15,901	-0,610	39,270	39,752	-1,227
3,0	2,743	2,761	-0,626	5,484	5,521	-0,679	10,957	11,042	-0,775	27,266	27,606	-1,246
3,5	2,012	2,028	-0,784	4,021	4,056	-0,892	8,033	8,113	-0,988	20,008	20,282	-1,368
4,0	1,540	1,553	-0,859	3,072	3,106	-1,101	6,135	6,211	-1,235	15,289	15,528	-1,564
4,5	1,218	1,227	-0,732	2,423	2,454	-1,264	4,835	4,908	-1,496	12,050	12,269	-1,817
5,0	0,992	0,994	-0,222	1,962	1,988	-1,316	3,907	3,975	-1,744	9,732	9,938	-2,113
5,5	0,829	0,821	0,902	1,624	1,643	-1,155	3,223	3,285	-1,941	8,018	8,213	-2,436
6,0	0,711	0,690	2,958	1,372	1,380	-0,631	2,706	2,761	-2,030	6,716	6,901	-2,768
6,5	0,627	0,529	15,600	1,181	1,176	0,423	2,308	2,352	-1,935	5,704	5,880	-3,086
7,0	0,569	0,489	14,027	1,037	1,014	2,224	1,997	2,028	-1,555	4,906	5,070	-3,359
7,5	0,532	0,466	12,379	0,929	0,883	4,951	1,753	1,767	-0,767	4,266	4,417	-3,547
8,0	0,511	0,456	10,844	0,851	0,831	2,330	1,562	1,553	0,562	3,747	3,882	-3,600
8,5	0,503	0,456	9,506	0,796	0,786	1,165	1,412	1,376	2,564	3,324	3,439	-3,456
9,0	0,506	0,464	8,329	0,760	0,757	0,370	1,296	1,227	5,341	2,977	3,067	-3,041
9,5	0,516	0,479	7,243	0,741	0,741	-0,030	1,209	1,266	-4,667	2,692	2,753	-2,277
10,0	0,532	0,500	6,162	0,734	0,735	-0,109	1,146	1,206	-5,200	2,458	2,485	-1,084
10,5	0,553	0,525	4,988	0,738	0,738	0,041	1,104	1,162	-5,320	2,267	2,254	0,612
11,0	0,577	0,555	3,685	0,750	0,748	0,277	1,078	1,132	-5,049	2,114	2,053	2,861
11,5	0,603	0,589	2,239	0,768	0,764	0,496	1,066	1,114	-4,462	1,992	1,879	5,686
12,0	0,630	0,626	0,621	0,791	0,786	0,589	1,066	1,105	-3,668	1,897	1,725	9,067
12,5	0,659	0,667	-1,136	0,817	0,813	0,524	1,075	1,105	-2,779	1,827	1,981	-8,452
13,0	0,645	0,648	-0,413	0,846	0,844	0,251	1,091	1,112	-1,900	1,776	1,916	-7,895
13,5	0,617	0,636	-3,025	0,877	0,879	-0,232	1,114	1,126	-1,112	1,743	1,866	-7,064
14,0	0,594	0,624	-5,092	0,910	0,918	-0,917	1,141	1,146	-0,476	1,725	1,829	-6,027
14,5	0,576	0,614	-6,592	0,944	0,961	-1,813	1,171	1,171	-0,029	1,719	1,802	-4,862
15,0	0,562	0,604	-7,525	0,941	0,905	3,858	1,204	1,201	0,210	1,723	1,786	-3,648
15,5	0,552	0,596	-7,904	0,902	0,889	1,448	1,239	1,236	0,233	1,736	1,778	-2,454
16,0	0,545	0,587	-7,813	0,868	0,873	-0,608	1,275	1,275	0,039	1,756	1,779	-1,339
16,5	0,540	0,580	-7,298	0,840	0,859	-2,299	1,312	1,317	-0,365	1,781	1,787	-0,348
17,0	0,538	0,572	-6,424	0,816	0,846	-3,608	1,350	1,364	-0,971	1,810	1,801	0,486
17,5	0,537	0,565	-5,263	0,797	0,833	-4,552	1,344	1,413	-5,186	1,843	1,822	1,143
18,0	0,538	0,559	-3,876	0,781	0,821	-5,136	1,291	1,232	4,563	1,879	1,849	1,611
18,5	0,540	0,553	-2,304	0,769	0,810	-5,386	1,245	1,212	2,659	1,917	1,881	1,884
19,0	0,543	0,547	-0,629	0,759	0,800	-5,349	1,204	1,192	0,988	1,956	1,917	1,961
19,5	0,547	0,541	1,127	0,752	0,790	-5,035	1,169	1,174	-0,443	1,996	1,959	1,847
20,0	0,552	0,536	2,926	0,746	0,780	-4,501	1,138	1,157	-1,630	2,036	2,005	1,545
20,5	0,557	0,530	4,731	0,743	0,771	-3,768	1,112	1,141	-2,579	2,077	2,055	1,061
21,0	0,562	0,525	6,508	0,741	0,762	-2,878	1,089	1,125	-3,295	2,118	2,110	0,402
21,5	0,559	0,520	6,913	0,740	0,754	-1,861	1,070	1,110	-3,791	2,113	2,168	-2,626
22,0	0,549	0,515	6,084	0,740	0,745	-0,746	1,053	1,096	-4,080	2,037	1,883	7,561
22,5	0,534	0,511	4,471	0,741	0,737	0,441	1,039	1,082	-4,181	1,969	1,853	5,856
23,0	0,524	0,506	3,522	0,742	0,730	1,677	1,026	1,069	-4,111	1,906	1,825	4,275
23,5	0,516	0,501	2,741	0,744	0,722	2,943	1,016	1,056	-3,888	1,850	1,797	2,821
24,0	0,508	0,497	2,111	0,746	0,715	4,222	1,008	1,043	-3,532	1,798	1,771	1,498
24,5	0,506	0,492	2,580	0,749	0,708	5,501	1,001	1,031	-3,061	1,751	1,746	0,308
25,0	0,494	0,488	1,258	0,751	0,701	6,767	0,995	1,019	-2,491	1,708	1,721	-0,747
25,5	0,489	0,484	1,033	0,754	0,694	8,010	0,990	1,008	-1,840	1,670	1,698	-1,670

$k = 0,05 \text{ [m}^{-1}\text{]}$												
	$t = 0,005 \text{ [m]}$			$t = 0,010 \text{ [m]}$			$t = 0,020 \text{ [m]}$			$t = 0,050 \text{ [m]}$		
L [m]	$f_{\text{ANSYS}}$ [Hz]	$f_{\text{FORMULA}}$ [Hz]	ERROR [%]									
26,0	0,484	0,479	0,899	0,737	0,687	6,784	0,986	0,997	-1,121	1,634	1,675	-2,463
26,5	0,479	0,475	0,879	0,721	0,680	5,648	0,982	0,986	-0,349	1,602	1,652	-3,129
27,0	0,475	0,471	0,917	0,706	0,673	4,624	0,979	0,975	0,466	1,573	1,631	-3,675
27,5	0,472	0,467	1,037	0,692	0,667	3,706	0,977	0,964	1,311	1,546	1,610	-4,104
28,0	0,468	0,462	1,219	0,680	0,660	2,893	0,975	0,953	2,178	1,522	1,589	-4,423
28,5	0,465	0,458	1,445	0,668	0,654	2,178	0,973	0,943	3,059	1,499	1,569	-4,639
29,0	0,462	0,454	1,717	0,657	0,647	1,559	0,971	0,933	3,946	1,478	1,549	-4,760
29,5	0,459	0,450	1,993	0,647	0,641	1,029	0,970	0,923	4,833	1,459	1,529	-4,791
30,0	0,456	0,446	2,317	0,638	0,634	0,583	0,968	0,913	5,714	1,442	1,510	-4,741
30,5	0,453	0,441	2,626	0,629	0,628	0,215	0,966	0,903	6,583	1,426	1,491	-4,615
31,0	0,450	0,437	2,942	0,621	0,621	-0,079	0,962	0,893	7,248	1,411	1,473	-4,421
31,5	0,447	0,433	3,244	0,613	0,615	-0,306	0,941	0,883	6,203	1,396	1,455	-4,166
32,0	0,439	0,429	2,412	0,606	0,609	-0,471	0,921	0,873	5,230	1,383	1,436	-3,854
32,5	0,431	0,424	1,600	0,599	0,602	-0,579	0,902	0,863	4,329	1,371	1,419	-3,492
33,0	0,424	0,420	0,880	0,592	0,596	-0,635	0,884	0,853	3,499	1,359	1,401	-3,086
33,5	0,417	0,416	0,212	0,586	0,589	-0,644	0,867	0,844	2,738	1,348	1,383	-2,639
34,0	0,410	0,411	-0,399	0,579	0,583	-0,612	0,851	0,834	2,047	1,337	1,366	-2,156
34,5	0,403	0,407	-0,948	0,573	0,576	-0,542	0,836	0,824	1,423	1,327	1,348	-1,641
35,0	0,397	0,402	-1,431	0,567	0,570	-0,438	0,821	0,814	0,864	1,317	1,331	-1,099
35,5	0,391	0,398	-1,869	0,562	0,563	-0,306	0,808	0,805	0,370	1,307	1,314	-0,532
36,0	0,385	0,393	-2,259	0,556	0,557	-0,148	0,794	0,795	-0,062	1,297	1,297	0,057
36,5	0,379	0,389	-2,597	0,550	0,550	0,031	0,782	0,785	-0,433	1,288	1,280	0,665
37,0	0,374	0,384	-2,881	0,545	0,543	0,228	0,769	0,775	-0,746	1,279	1,262	1,289
37,5	0,368	0,380	-3,108	0,539	0,537	0,439	0,758	0,765	-1,001	1,270	1,245	1,928
38,0	0,363	0,375	-3,302	0,534	0,530	0,662	0,746	0,755	-1,202	1,261	1,228	2,580
38,5	0,358	0,370	-3,463	0,528	0,523	0,892	0,736	0,745	-1,349	1,252	1,211	3,242
39,0	0,353	0,366	-3,588	0,522	0,516	1,128	0,725	0,736	-1,444	1,243	1,194	3,914
39,5	0,348	0,361	-3,675	0,517	0,510	1,366	0,715	0,726	-1,490	1,234	1,177	4,593
40,0	0,343	0,356	-3,730	0,508	0,503	1,125	0,705	0,715	-1,487	1,225	1,160	5,279

**Table C2** Comparison of ANSYS and formula frequencies for Case 2.

L [m]	$k = 0,10 \text{ [m}^{-1}\text{]}$											
	$t = 0,0025 \text{ [m]}$			$t = 0,0050 \text{ [m]}$			$t = 0,0100 \text{ [m]}$			$t = 0,0500 \text{ [m]}$		
	$f_{\text{ANSYS}}$ [Hz]	$f_{\text{FORMULA}}$ [Hz]	ERROR [%]	$f_{\text{ANSYS}}$ [Hz]	$f_{\text{FORMULA}}$ [Hz]	ERROR [%]	$f_{\text{ANSYS}}$ [Hz]	$f_{\text{FORMULA}}$ [Hz]	ERROR [%]	$f_{\text{ANSYS}}$ [Hz]	$f_{\text{FORMULA}}$ [Hz]	ERROR [%]
0,2	309,531	310,564	-0,33	614,599	621,128	-1,06	1207,57	1242,26	-2,87	4839,54	6211,28	-28,34
0,4	77,553	77,641	-0,11	154,708	155,282	-0,37	307,185	310,564	-1,10	1405,58	1552,82	-10,48
0,6	34,465	34,507	-0,12	68,843	69,014	-0,25	137,130	138,028	-0,66	651,301	690,142	-5,96
0,8	19,374	19,410	-0,19	38,718	38,820	-0,26	77,239	77,641	-0,52	372,879	388,205	-4,11
1,0	12,387	12,423	-0,29	24,761	24,845	-0,34	49,435	49,690	-0,52	240,798	248,451	-3,18
1,2	8,591	8,627	-0,41	17,175	17,254	-0,46	34,306	34,507	-0,59	168,047	172,535	-2,67
1,4	6,303	6,338	-0,55	12,601	12,676	-0,60	25,175	25,352	-0,70	123,792	126,761	-2,40
1,6	4,819	4,853	-0,69	9,632	9,705	-0,76	19,246	19,410	-0,86	94,893	97,051	-2,27
1,8	3,803	3,834	-0,81	7,597	7,668	-0,94	15,179	15,336	-1,04	74,994	76,682	-2,25
2,0	3,079	3,106	-0,86	6,144	6,211	-1,10	12,271	12,423	-1,24	60,712	62,113	-2,31
2,2	2,547	2,567	-0,78	5,071	5,133	-1,24	10,121	10,267	-1,44	50,118	51,333	-2,42
2,4	2,146	2,157	-0,49	4,257	4,313	-1,32	8,487	8,627	-1,65	42,045	43,134	-2,59
2,6	1,840	1,838	0,13	3,629	3,675	-1,28	7,218	7,351	-1,83	35,754	36,753	-2,79
2,8	1,604	1,585	1,23	3,135	3,169	-1,08	6,216	6,338	-1,97	30,756	31,690	-3,04
3,0	1,422	1,380	2,96	2,743	2,761	-0,63	5,411	5,521	-2,03	26,721	27,606	-3,31
3,2	1,283	1,213	5,47	2,430	2,426	0,16	4,759	4,853	-1,97	23,418	24,263	-3,61
3,4	1,179	1,006	14,68	2,180	2,149	1,40	4,225	4,298	-1,75	20,682	21,492	-3,92
3,6	1,104	0,957	13,36	1,980	1,917	3,19	3,785	3,834	-1,30	18,392	19,171	-4,23
3,8	1,053	0,926	12,05	1,823	1,721	5,62	3,422	3,441	-0,55	16,457	17,206	-4,55
4,0	1,022	0,911	10,84	1,701	1,662	2,33	3,123	3,106	0,56	14,810	15,528	-4,85
4,2	1,008	0,910	9,75	1,610	1,588	1,38	2,878	2,817	2,11	13,398	14,085	-5,12
4,4	1,008	0,919	8,78	1,545	1,535	0,64	2,677	2,567	4,13	12,182	12,833	-5,35
4,6	1,018	0,938	7,89	1,501	1,499	0,16	2,516	2,348	6,68	11,128	11,742	-5,51
4,8	1,038	0,965	7,03	1,477	1,478	-0,07	2,390	2,504	-4,81	10,213	10,783	-5,59
5,0	1,065	0,999	6,16	1,468	1,470	-0,11	2,293	2,412	-5,20	9,415	9,938	-5,56
5,2	1,097	1,039	5,23	1,473	1,473	0,00	2,221	2,340	-5,33	8,718	9,188	-5,39
5,4	1,133	1,086	4,22	1,488	1,486	0,18	2,173	2,286	-5,20	8,110	8,520	-5,06
5,6	1,173	1,137	3,12	1,513	1,507	0,37	2,143	2,247	-4,85	7,579	7,923	-4,53
5,8	1,216	1,193	1,92	1,544	1,536	0,52	2,131	2,223	-4,31	7,116	7,386	-3,79
6,0	1,261	1,253	0,62	1,581	1,572	0,59	2,132	2,210	-3,67	6,714	6,901	-2,79
6,2	1,307	1,317	-0,77	1,623	1,614	0,55	2,145	2,209	-2,96	6,366	6,463	-1,53
6,4	1,317	1,307	0,78	1,669	1,662	0,38	2,168	2,217	-2,24	6,066	6,066	0,01
6,6	1,267	1,286	-1,52	1,717	1,716	0,08	2,200	2,234	-1,57	5,810	5,704	1,84
6,8	1,224	1,267	-3,49	1,768	1,774	-0,35	2,238	2,259	-0,97	5,594	5,373	3,95
7,0	1,188	1,249	-5,10	1,820	1,837	-0,92	2,281	2,292	-0,48	5,413	5,070	6,33
7,2	1,159	1,232	-6,34	1,874	1,904	-1,61	2,329	2,331	-0,10	5,264	4,793	8,96
7,4	1,134	1,216	-7,21	1,919	1,976	-2,97	2,381	2,377	0,14	5,144	5,591	-8,68
7,6	1,115	1,202	-7,74	1,850	1,797	2,85	2,435	2,429	0,25	5,050	5,454	-8,00
7,8	1,100	1,188	-7,93	1,789	1,771	1,01	2,492	2,487	0,21	4,978	5,337	-7,21
8,0	1,089	1,175	-7,82	1,736	1,746	-0,61	2,550	2,549	0,04	4,927	5,239	-6,32
8,2	1,082	1,162	-7,44	1,690	1,723	-1,99	2,610	2,617	-0,27	4,894	5,157	-5,37
8,4	1,077	1,150	-6,82	1,650	1,702	-3,13	2,670	2,689	-0,70	4,877	5,090	-4,38
8,6	1,074	1,139	-6,00	1,616	1,681	-4,03	2,732	2,766	-1,27	4,873	5,038	-3,38
8,8	1,074	1,128	-5,00	1,587	1,661	-4,70	2,665	2,499	6,25	4,881	4,998	-2,39
9,0	1,076	1,118	-3,87	1,562	1,643	-5,14	2,582	2,464	4,56	4,900	4,971	-1,45
9,2	1,079	1,108	-2,63	1,542	1,625	-5,37	2,507	2,431	3,02	4,927	4,955	-0,56
9,4	1,084	1,098	-1,31	1,525	1,608	-5,40	2,440	2,400	1,63	4,962	4,950	0,25
9,6	1,090	1,089	0,06	1,512	1,591	-5,25	2,379	2,370	0,39	5,003	4,955	0,97
9,8	1,096	1,080	1,48	1,501	1,575	-4,95	2,325	2,341	-0,70	5,050	4,969	1,60
10,0	1,103	1,071	2,92	1,493	1,560	-4,50	2,277	2,314	-1,63	5,101	4,992	2,13
10,2	1,111	1,063	4,36	1,487	1,545	-3,93	2,234	2,288	-2,41	5,155	5,024	2,55

L [m]	$k = 0,10 \text{ [m}^{-1}\text{]}$											
	$t = 0,0025 \text{ [m]}$			$t = 0,0050 \text{ [m]}$			$t = 0,0100 \text{ [m]}$			$t = 0,0500 \text{ [m]}$		
	$f_{\text{ANSYS}}$ [Hz]	$f_{\text{FORMULA}}$ [Hz]	ERROR [%]	$f_{\text{ANSYS}}$ [Hz]	$f_{\text{FORMULA}}$ [Hz]	ERROR [%]	$f_{\text{ANSYS}}$ [Hz]	$f_{\text{FORMULA}}$ [Hz]	ERROR [%]	$f_{\text{ANSYS}}$ [Hz]	$f_{\text{FORMULA}}$ [Hz]	ERROR [%]
10,4	1,119	1,054	5,80	1,483	1,531	-3,25	2,196	2,262	-3,04	5,213	5,064	2,86
10,6	1,128	1,046	7,22	1,481	1,517	-2,48	2,162	2,238	-3,52	5,272	5,111	3,06
10,8	1,112	1,038	6,63	1,480	1,504	-1,64	2,132	2,214	-3,86	5,334	5,166	3,15
11,0	1,092	1,031	5,60	1,480	1,491	-0,75	2,106	2,191	-4,08	5,397	5,228	3,12
11,2	1,073	1,023	4,68	1,481	1,478	0,20	2,082	2,169	-4,18	5,460	5,297	2,99
11,4	1,057	1,016	3,88	1,483	1,466	1,18	2,062	2,148	-4,16	5,524	5,373	2,75
11,6	1,041	1,008	3,18	1,486	1,453	2,18	2,044	2,127	-4,04	5,589	5,454	2,40
11,8	1,028	1,001	2,59	1,489	1,441	3,20	2,029	2,107	-3,83	5,653	5,543	1,95
12,0	1,015	0,994	2,10	1,493	1,430	4,22	2,015	2,087	-3,53	5,717	5,637	1,40
12,2	1,004	0,987	1,70	1,497	1,418	5,25	2,004	2,067	-3,16	5,780	5,737	0,75
12,4	0,993	0,980	1,39	1,501	1,407	6,26	1,994	2,048	-2,73	5,843	5,843	0,00
12,6	0,984	0,973	1,16	1,505	1,396	7,27	1,985	2,029	-2,24	5,842	5,955	-1,93
12,8	0,975	0,966	1,00	1,501	1,384	7,77	1,978	2,011	-1,70	5,685	5,157	9,30
13,0	0,968	0,959	0,90	1,474	1,374	6,78	1,971	1,993	-1,12	5,538	5,092	8,06
13,2	0,960	0,952	0,87	1,448	1,363	5,87	1,965	1,975	-0,51	5,399	5,028	6,86
13,4	0,954	0,945	0,89	1,423	1,352	5,02	1,961	1,958	0,14	5,268	4,967	5,71
13,6	0,948	0,938	0,96	1,401	1,341	4,24	1,956	1,941	0,80	5,144	4,907	4,61
13,8	0,942	0,932	1,07	1,380	1,331	3,54	1,953	1,924	1,48	5,028	4,849	3,56
14,0	0,936	0,925	1,22	1,360	1,320	2,89	1,949	1,907	2,18	4,918	4,792	2,56
14,2	0,931	0,918	1,40	1,341	1,310	2,31	1,946	1,890	2,88	4,814	4,736	1,62
14,4	0,926	0,912	1,60	1,323	1,300	1,80	1,944	1,874	3,59	4,716	4,681	0,74
14,6	0,922	0,905	1,82	1,307	1,289	1,34	1,941	1,858	4,30	4,624	4,628	-0,09
14,8	0,917	0,898	2,06	1,291	1,279	0,93	1,938	1,841	5,01	4,536	4,575	-0,87
15,0	0,912	0,891	2,31	1,276	1,269	0,58	1,936	1,825	5,71	4,453	4,524	-1,59
15,2	0,908	0,884	2,56	1,262	1,258	0,28	1,933	1,809	6,41	4,375	4,473	-2,25
15,4	0,903	0,878	2,81	1,248	1,248	0,03	1,930	1,793	7,10	4,300	4,423	-2,86
15,6	0,898	0,871	3,06	1,236	1,238	-0,18	1,908	1,778	6,82	4,230	4,374	-3,42
15,8	0,892	0,864	3,09	1,223	1,228	-0,34	1,874	1,762	6,00	4,163	4,326	-3,92
16,0	0,878	0,857	2,40	1,212	1,217	-0,47	1,842	1,746	5,23	4,099	4,278	-4,37
16,2	0,866	0,850	1,76	1,200	1,207	-0,56	1,812	1,730	4,50	4,039	4,231	-4,76
16,4	0,853	0,843	1,15	1,189	1,197	-0,62	1,783	1,715	3,82	3,981	4,185	-5,11
16,6	0,841	0,836	0,59	1,179	1,186	-0,64	1,755	1,699	3,19	3,926	4,139	-5,41
16,8	0,830	0,829	0,07	1,169	1,176	-0,64	1,728	1,683	2,59	3,874	4,093	-5,66
17,0	0,819	0,822	-0,41	1,159	1,166	-0,61	1,703	1,668	2,05	3,824	4,048	-5,86
17,2	0,809	0,815	-0,85	1,149	1,155	-0,56	1,678	1,652	1,54	3,776	4,003	-6,02
17,4	0,798	0,808	-1,25	1,139	1,145	-0,48	1,654	1,637	1,08	3,730	3,959	-6,14
17,6	0,788	0,801	-1,62	1,130	1,135	-0,39	1,632	1,621	0,66	3,686	3,915	-6,21
17,8	0,779	0,794	-1,96	1,121	1,124	-0,28	1,610	1,605	0,28	3,644	3,871	-6,24
18,0	0,769	0,787	-2,26	1,112	1,113	-0,15	1,589	1,590	-0,06	3,603	3,828	-6,24
18,2	0,760	0,780	-2,53	1,103	1,103	-0,01	1,568	1,574	-0,36	3,564	3,785	-6,19
18,4	0,751	0,772	-2,77	1,094	1,092	0,15	1,549	1,558	-0,63	3,527	3,742	-6,11
18,6	0,743	0,765	-2,98	1,085	1,082	0,31	1,529	1,542	-0,85	3,490	3,700	-6,00
18,8	0,734	0,757	-3,16	1,076	1,071	0,48	1,511	1,527	-1,05	3,455	3,657	-5,85
19,0	0,726	0,750	-3,31	1,067	1,060	0,66	1,493	1,511	-1,20	3,421	3,615	-5,67
19,2	0,718	0,742	-3,44	1,058	1,049	0,85	1,475	1,495	-1,32	3,388	3,573	-5,46
19,4	0,710	0,735	-3,55	1,049	1,038	1,03	1,458	1,479	-1,41	3,356	3,531	-5,21
19,6	0,702	0,727	-3,63	1,040	1,027	1,22	1,442	1,463	-1,47	3,325	3,489	-4,94
19,8	0,694	0,720	-3,69	1,031	1,016	1,41	1,426	1,447	-1,49	3,295	3,448	-4,65
20,0	0,686	0,712	-3,73	1,017	1,005	1,12	1,410	1,431	-1,49	3,265	3,406	-4,32

**Table C3** Comparison of ANSYS and formula frequencies for Case 3.

L [m]	$k = 0,20 \text{ [m}^{-1}\text{]}$											
	$t = 0,0015 \text{ [m]}$			$t = 0,0050 \text{ [m]}$			$t = 0,0100 \text{ [m]}$			$t = 0,0500 \text{ [m]}$		
	$f_{\text{ANSYS}}$ [Hz]	$f_{\text{FORMULA}}$ [Hz]	ERROR [%]	$f_{\text{ANSYS}}$ [Hz]	$f_{\text{FORMULA}}$ [Hz]	ERROR [%]	$f_{\text{ANSYS}}$ [Hz]	$f_{\text{FORMULA}}$ [Hz]	ERROR [%]	$f_{\text{ANSYS}}$ [Hz]	$f_{\text{FORMULA}}$ [Hz]	ERROR [%]
0,2	186,049	186,338	-0,16	614,370	621,128	-1,10	1207,12	1242,26	-2,91	4837,67	6211,28	-28,39
0,4	46,492	46,585	-0,20	154,477	155,282	-0,52	306,727	310,564	-1,25	1403,49	1552,82	-10,64
0,6	20,617	20,704	-0,42	68,613	69,014	-0,59	136,671	138,028	-0,99	649,134	690,142	-6,32
0,8	11,564	11,646	-0,71	38,491	38,820	-0,86	76,781	77,641	-1,12	370,677	388,205	-4,73
1,0	7,384	7,454	-0,94	24,542	24,845	-1,24	48,983	49,690	-1,44	238,582	248,451	-4,14
1,2	5,136	5,176	-0,79	16,974	17,254	-1,65	33,868	34,507	-1,89	165,830	172,535	-4,04
1,4	3,818	3,803	0,40	12,431	12,676	-1,97	24,762	25,352	-2,38	121,585	126,761	-4,26
1,6	3,021	2,912	3,61	9,517	9,705	-1,97	18,874	19,410	-2,84	92,708	97,051	-4,68
1,8	2,552	2,286	10,42	7,570	7,668	-1,30	14,873	15,336	-3,12	72,844	76,682	-5,27
2,0	2,309	2,123	8,08	6,246	6,211	0,56	12,063	12,423	-2,98	58,617	62,113	-5,96
2,2	2,226	2,084	6,36	5,355	5,133	4,13	10,053	10,267	-2,12	48,102	51,333	-6,72
2,4	2,252	2,135	5,19	4,779	5,009	-4,80	8,611	8,627	-0,18	40,136	43,134	-7,47
2,6	2,350	2,252	4,14	4,443	4,680	-5,33	7,592	7,351	3,18	33,994	36,753	-8,12
2,8	2,493	2,422	2,86	4,287	4,494	-4,85	6,898	6,338	8,12	29,185	31,690	-8,58
3,0	2,664	2,633	1,16	4,264	4,420	-3,67	6,459	6,973	-7,95	25,390	27,606	-8,73
3,2	2,852	2,881	-0,99	4,336	4,434	-2,24	6,219	6,652	-6,96	22,385	24,263	-8,39
3,4	2,825	2,819	0,21	4,475	4,519	-0,97	6,131	6,460	-5,37	20,010	21,492	-7,41
3,6	2,645	2,737	-3,50	4,658	4,663	-0,10	6,156	6,372	-3,51	18,147	19,171	-5,64
3,8	2,517	2,666	-5,91	4,870	4,858	0,25	6,264	6,371	-1,71	16,706	17,206	-2,99
4,0	2,431	2,602	-7,03	5,101	5,098	0,04	6,431	6,444	-0,20	15,616	15,528	0,56
4,2	2,378	2,545	-7,01	5,341	5,378	-0,70	6,636	6,579	0,86	14,817	14,085	4,94
4,4	2,351	2,494	-6,05	5,330	4,997	6,25	6,868	6,771	1,42	14,258	15,368	-7,78
4,6	2,344	2,446	-4,38	5,014	4,862	3,02	7,117	7,012	1,47	13,895	14,736	-6,05
4,8	2,350	2,402	-2,22	4,759	4,740	0,39	7,373	7,298	1,02	13,689	14,257	-4,15
5,0	2,367	2,361	0,24	4,554	4,628	-1,63	7,633	7,627	0,09	13,607	13,909	-2,22
5,2	2,391	2,323	2,85	4,392	4,525	-3,03	7,385	6,833	7,47	13,620	13,678	-0,42
5,4	2,419	2,286	5,50	4,264	4,429	-3,86	6,985	6,659	4,67	13,706	13,549	1,14
5,6	2,433	2,251	7,49	4,165	4,339	-4,18	6,646	6,497	2,24	13,845	13,512	2,40
5,8	2,345	2,217	5,46	4,089	4,254	-4,04	6,360	6,347	0,20	14,022	13,559	3,30
6,0	2,271	2,184	3,83	4,031	4,173	-3,53	6,117	6,205	-1,44	14,224	13,682	3,81
6,2	2,209	2,153	2,58	3,987	4,096	-2,73	5,912	6,072	-2,70	14,444	13,876	3,93
6,4	2,157	2,121	1,67	3,955	4,022	-1,70	5,739	5,945	-3,59	14,672	14,136	3,65
6,6	2,113	2,090	1,06	3,931	3,951	-0,51	5,592	5,824	-4,15	14,903	14,457	2,99
6,8	2,075	2,060	0,72	3,913	3,882	0,80	5,467	5,707	-4,40	15,132	14,839	1,94
7,0	2,042	2,030	0,60	3,899	3,814	2,18	5,360	5,595	-4,38	15,357	15,276	0,52
7,2	2,013	1,999	0,66	3,887	3,748	3,59	5,268	5,486	-4,14	15,573	15,769	-1,25
7,4	1,986	1,969	0,85	3,877	3,683	5,01	5,188	5,381	-3,71	15,780	16,315	-3,39
7,6	1,962	1,939	1,16	3,866	3,619	6,41	5,118	5,277	-3,11	15,100	13,715	9,17
7,8	1,939	1,909	1,53	3,815	3,555	6,82	5,055	5,176	-2,39	14,398	13,374	7,11
8,0	1,916	1,879	1,94	3,685	3,492	5,23	4,998	5,076	-1,56	13,759	13,046	5,18
8,2	1,893	1,848	2,36	3,566	3,429	3,82	4,946	4,978	-0,65	13,176	12,729	3,39
8,4	1,859	1,817	2,26	3,456	3,367	2,59	4,897	4,881	0,33	12,642	12,422	1,74
8,6	1,805	1,786	1,06	3,356	3,304	1,54	4,850	4,784	1,35	12,154	12,124	0,25
8,8	1,755	1,755	0,01	3,263	3,242	0,66	4,804	4,688	2,40	11,705	11,833	-1,09
9,0	1,708	1,723	-0,88	3,177	3,179	-0,06	4,758	4,593	3,48	11,292	11,549	-2,28
9,2	1,664	1,691	-1,63	3,097	3,116	-0,63	4,713	4,498	4,57	10,911	11,270	-3,30
9,4	1,622	1,658	-2,25	3,022	3,053	-1,05	4,667	4,403	5,66	10,558	10,997	-4,16
9,6	1,582	1,625	-2,73	2,951	2,990	-1,32	4,607	4,308	6,50	10,231	10,728	-4,86
9,8	1,544	1,592	-3,09	2,884	2,926	-1,47	4,455	4,213	5,44	9,927	10,463	-5,40
10,0	1,508	1,558	-3,34	2,820	2,862	-1,49	4,312	4,117	4,53	9,643	10,201	-5,78

**Table C4** Comparison of ANSYS and formula frequencies for Case 4.

L [m]	$k = 0,30 \text{ [m}^{-1}\text{]}$											
	$t = 0,001 \text{ [m]}$			$t = 0,005 \text{ [m]}$			$t = 0,010 \text{ [m]}$			$t = 0,050 \text{ [m]}$		
	$f_{\text{ANSYS}}$ [Hz]	$f_{\text{FORMULA}}$ [Hz]	ERROR [%]	$f_{\text{ANSYS}}$ [Hz]	$f_{\text{FORMULA}}$ [Hz]	ERROR [%]	$f_{\text{ANSYS}}$ [Hz]	$f_{\text{FORMULA}}$ [Hz]	ERROR [%]	$f_{\text{ANSYS}}$ [Hz]	$f_{\text{FORMULA}}$ [Hz]	ERROR [%]
0,2	124,050	124,226	-0,14	613,988	621,128	-1,16	1206,38	1242,26	-2,97	4834,54	6211,28	-28,48
0,4	30,926	31,056	-0,42	154,094	155,282	-0,77	305,966	310,564	-1,50	1400,03	1552,82	-10,91
0,6	13,686	13,803	-0,85	68,237	69,014	-1,14	135,915	138,028	-1,55	645,550	690,142	-6,91
0,8	7,703	7,764	-0,79	38,141	38,820	-1,78	76,044	77,641	-2,10	367,059	388,205	-5,76
1,0	5,054	4,969	1,68	24,257	24,845	-2,42	48,296	49,690	-2,89	234,977	248,451	-5,73
1,2	3,828	3,429	10,42	16,825	17,254	-2,55	33,284	34,507	-3,67	162,281	172,535	-6,32
1,4	3,377	3,136	7,13	12,530	12,676	-1,16	24,367	25,352	-4,04	118,143	126,761	-7,29
1,6	3,378	3,203	5,19	10,016	9,705	3,10	18,792	19,410	-3,29	89,446	97,051	-8,50
1,8	3,625	3,497	3,54	8,638	9,257	-7,17	15,264	15,336	-0,48	69,858	76,682	-9,77
2,0	3,996	3,950	1,16	8,026	8,545	-6,46	13,105	12,423	5,21	56,036	62,113	-10,84
2,2	4,409	4,525	-2,63	7,923	8,257	-4,21	11,910	12,922	-8,50	46,085	51,333	-11,39
2,4	3,967	4,106	-3,50	8,140	8,276	-1,67	11,394	12,122	-6,39	38,871	43,134	-10,97
2,6	3,704	3,950	-6,63	8,545	8,529	0,19	11,340	11,737	-3,50	33,679	36,753	-9,13
2,8	3,568	3,818	-7,01	9,052	8,968	0,93	11,584	11,670	-0,74	30,011	31,690	-5,59
3,0	3,518	3,704	-5,29	9,609	9,563	0,48	12,008	11,857	1,26	27,525	27,606	-0,29
3,2	3,525	3,604	-2,22	9,848	10,294	-4,53	12,533	12,253	2,23	25,944	24,263	6,48
3,4	3,568	3,513	1,54	9,029	8,720	3,43	13,107	12,830	2,11	25,044	26,259	-4,85
3,6	3,629	3,429	5,50	8,410	8,409	0,01	13,697	13,566	0,96	24,639	25,139	-2,03
3,8	3,581	3,351	6,43	7,943	8,129	-2,34	13,447	12,319	8,38	24,582	24,450	0,54
4,0	3,407	3,277	3,83	7,595	7,875	-3,68	12,425	11,863	4,52	24,757	24,126	2,55
4,2	3,273	3,205	2,08	7,336	7,639	-4,14	11,600	11,449	1,30	25,079	24,119	3,83
4,4	3,169	3,136	1,06	7,142	7,419	-3,88	10,931	11,067	-1,24	25,488	24,393	4,29
4,6	3,087	3,067	0,63	6,997	7,211	-3,06	10,388	10,711	-3,10	25,938	24,920	3,93
4,8	3,019	2,999	0,65	6,884	7,011	-1,84	9,944	10,375	-4,33	26,398	25,679	2,73
5,0	2,961	2,931	0,99	6,793	6,818	-0,36	9,578	10,056	-4,99	26,847	26,655	0,71
5,2	2,908	2,863	1,53	6,717	6,630	1,29	9,271	9,750	-5,16	27,270	27,839	-2,09
5,4	2,856	2,795	2,15	6,647	6,446	3,02	9,010	9,453	-4,92	27,656	29,223	-5,66
5,6	2,789	2,726	2,27	6,579	6,264	4,78	8,785	9,165	-4,33	26,531	24,079	9,24
5,8	2,670	2,656	0,52	6,509	6,084	6,53	8,585	8,882	-3,46	24,800	23,168	6,58
6,0	2,562	2,584	-0,88	6,215	5,904	5,00	8,404	8,603	-2,37	23,267	22,296	4,17
6,2	2,464	2,512	-1,96	5,920	5,724	3,31	8,236	8,327	-1,11	21,904	21,457	2,04
6,4	2,373	2,438	-2,73	5,655	5,544	1,97	8,078	8,053	0,30	20,688	20,644	0,21
6,6	2,289	2,363	-3,23	5,415	5,363	0,96	7,925	7,780	1,82	19,598	19,854	-1,31
6,8	2,209	2,286	-3,47	5,196	5,181	0,29	7,775	7,507	3,44	18,617	19,083	-2,51

**Table C5** Comparison of ANSYS and formula frequencies for Case 5.

L [m]	$k = 0,40 \text{ [m}^{-1}\text{]}$											
	$t = 0,001 \text{ [m]}$			$t = 0,005 \text{ [m]}$			$t = 0,010 \text{ [m]}$			$t = 0,050 \text{ [m]}$		
	$f_{\text{ANSYS}}$ [Hz]	$f_{\text{FORMULA}}$ [Hz]	ERROR [%]	$f_{\text{ANSYS}}$ [Hz]	$f_{\text{FORMULA}}$ [Hz]	ERROR [%]	$f_{\text{ANSYS}}$ [Hz]	$f_{\text{FORMULA}}$ [Hz]	ERROR [%]	$f_{\text{ANSYS}}$ [Hz]	$f_{\text{FORMULA}}$ [Hz]	ERROR [%]
0,2	123,942	124,226	-0,23	613,453	621,128	-1,25	1205,33	1242,26	-3,06	4830,17	6211,28	-28,59
0,4	30,828	31,056	-0,74	153,563	155,282	-1,12	304,908	310,564	-1,85	1395,20	1552,82	-11,30
0,6	13,649	13,803	-1,13	67,736	69,014	-1,89	134,881	138,028	-2,33	640,592	690,142	-7,74
0,8	7,874	7,764	1,40	37,747	38,820	-2,84	75,091	77,641	-3,40	362,108	388,205	-7,21
1,0	5,701	5,446	4,47	24,126	24,845	-2,98	47,545	49,690	-4,51	230,138	248,451	-7,96
1,2	5,204	5,091	2,16	17,223	17,254	-0,18	32,944	34,507	-4,74	157,683	172,535	-9,42
1,4	5,531	5,435	1,73	13,797	12,676	8,12	24,744	25,352	-2,46	113,971	126,761	-11,22
1,6	6,216	6,205	0,17	12,438	13,304	-6,96	20,247	19,410	4,13	85,962	97,051	-12,90
1,8	6,627	6,485	2,15	12,313	12,744	-3,51	18,102	19,580	-8,17	67,408	76,682	-13,76
2,0	5,892	6,134	-4,11	12,861	12,887	-0,20	17,454	18,266	-4,65	55,021	62,113	-12,89
2,2	5,519	5,855	-6,09	13,737	13,541	1,42	17,698	17,843	-0,82	46,907	51,333	-9,44
2,4	5,374	5,623	-4,62	14,747	14,597	1,02	18,424	18,079	1,87	41,856	43,134	-3,05
2,6	5,365	5,422	-1,08	14,770	13,666	7,47	19,378	18,833	2,81	38,979	36,753	5,71
2,8	5,426	5,244	3,35	13,293	12,995	2,24	20,414	20,019	1,93	37,598	38,661	-2,83
3,0	5,516	5,080	7,90	12,235	12,411	-1,44	21,001	21,583	-2,77	37,195	36,961	0,63
3,2	5,151	4,925	4,38	11,478	11,890	-3,59	18,913	17,963	5,03	37,388	36,200	3,18
3,4	4,871	4,777	1,93	10,934	11,415	-4,40	17,297	17,134	0,94	37,912	36,224	4,45
3,6	4,658	4,632	0,54	10,536	10,973	-4,14	16,035	16,379	-2,14	38,593	36,927	4,32
3,8	4,488	4,489	-0,01	10,236	10,554	-3,11	15,042	15,679	-4,23	39,317	38,236	2,75
4,0	4,347	4,345	0,04	9,997	10,152	-1,56	14,247	15,018	-5,42	40,014	40,102	-0,22
4,2	4,221	4,201	0,48	9,793	9,761	0,33	13,598	14,388	-5,81	40,639	42,493	-4,56
4,4	4,100	4,054	1,12	9,608	9,377	2,40	13,056	13,778	-5,53	41,166	45,391	-10,26
4,6	3,968	3,904	1,61	9,426	8,995	4,57	12,591	13,183	-4,71	37,883	34,834	8,05
4,8	3,744	3,752	-0,22	9,214	8,615	6,50	12,179	12,598	-3,44	34,833	33,037	5,16
5,0	3,543	3,596	-1,49	8,625	8,234	4,53	11,805	12,018	-1,80	32,194	31,317	2,73

**Table C6** Comparison of ANSYS and formula frequencies for Case 6.

L [m]	$k = 0,50 \text{ [m}^{-1}\text{]}$											
	$t = 0,0005 \text{ [m]}$			$t = 0,0010 \text{ [m]}$			$t = 0,0050 \text{ [m]}$			$t = 0,0100 \text{ [m]}$		
	$f_{\text{ANSYS}}$ [Hz]	$f_{\text{FORMULA}}$ [Hz]	ERROR [%]	$f_{\text{ANSYS}}$ [Hz]	$f_{\text{FORMULA}}$ [Hz]	ERROR [%]	$f_{\text{ANSYS}}$ [Hz]	$f_{\text{FORMULA}}$ [Hz]	ERROR [%]	$f_{\text{ANSYS}}$ [Hz]	$f_{\text{FORMULA}}$ [Hz]	ERROR [%]
0,2	123,804	124,226	-0,34	612,768	621,128	-1,36	1203,99	1242,26	-3,18	4824,56	6211,28	-28,74
0,4	30,718	31,056	-1,10	152,890	155,282	-1,56	303,560	310,564	-2,31	1389,04	1552,82	-11,79
0,6	13,716	13,803	-0,63	67,155	69,014	-2,77	133,605	138,028	-3,31	634,320	690,142	-8,80
0,8	8,507	8,309	2,33	37,471	38,820	-3,60	74,050	77,641	-4,85	355,951	388,205	-9,06
1,0	7,342	7,350	-0,11	24,579	24,845	-1,08	47,074	49,690	-5,56	224,323	248,451	-10,76
1,2	7,906	7,859	0,59	18,974	17,254	9,07	33,570	34,507	-2,79	152,535	172,535	-13,11
1,4	9,101	9,184	-0,92	17,246	18,286	-6,03	27,066	25,352	6,33	109,978	126,761	-15,26
1,6	8,679	8,732	-0,61	17,555	17,790	-1,34	24,636	26,194	-6,32	83,766	97,051	-15,86
1,8	7,812	8,213	-5,14	18,790	18,487	1,61	24,500	24,855	-1,45	67,706	76,682	-13,26
2,0	7,465	7,801	-4,50	20,364	20,050	1,54	25,504	24,961	2,13	58,368	62,113	-6,42
2,2	7,399	7,454	-0,75	20,373	18,833	7,56	26,983	26,141	3,12	53,509	51,333	4,07
2,4	7,464	7,148	4,22	17,980	17,711	1,50	28,585	28,185	1,40	51,503	52,178	-1,31
2,6	7,368	6,868	6,78	16,344	16,746	-2,46	27,689	25,458	8,06	51,154	49,874	2,50
2,8	6,798	6,602	2,89	15,216	15,889	-4,42	24,589	23,959	2,56	51,678	49,312	4,58
3,0	6,380	6,343	0,58	14,419	15,103	-4,74	22,266	22,619	-1,59	52,587	50,198	4,54
3,2	6,058	6,087	-0,47	13,832	14,365	-3,85	20,496	21,391	-4,37	53,589	52,341	2,33
3,4	5,794	5,829	-0,61	13,368	13,657	-2,16	19,119	20,240	-5,86	54,519	55,625	-2,03
3,6	5,559	5,567	-0,15	12,974	12,966	0,06	18,017	19,140	-6,24	55,285	59,986	-8,50
3,8	5,336	5,300	0,66	12,610	12,284	2,58	17,105	18,075	-5,67	53,834	48,396	10,10
4,0	5,084	5,027	1,13	12,252	11,605	5,28	16,326	17,031	-4,32	48,472	45,208	6,73

**Table C7** Comparison of ANSYS and formula frequencies for Case 7.

L [m]	$k = 1,00 \text{ [m}^{-1}\text{]}$											
	$t = 0,001 \text{ [m]}$			$t = 0,005 \text{ [m]}$			$t = 0,010 \text{ [m]}$			$t = 0,050 \text{ [m]}$		
	$f_{\text{ANSYS}}$ [Hz]	$f_{\text{FORMULA}}$ [Hz]	ERROR [%]	$f_{\text{ANSYS}}$ [Hz]	$f_{\text{FORMULA}}$ [Hz]	ERROR [%]	$f_{\text{ANSYS}}$ [Hz]	$f_{\text{FORMULA}}$ [Hz]	ERROR [%]	$f_{\text{ANSYS}}$ [Hz]	$f_{\text{FORMULA}}$ [Hz]	ERROR [%]
0,05	991,003	993,804	-0,28	1971,53	1987,61	-0,82	9231,51	9938,04	-7,65	16474,6	19876,1	-20,65
0,10	247,609	248,451	-0,34	494,347	496,902	-0,52	2407,98	2484,51	-3,18	4605,08	4969,02	-7,90
0,15	109,678	110,423	-0,68	219,147	220,845	-0,77	1079,18	1104,23	-2,32	2103,30	2208,45	-5,00
0,20	61,436	62,113	-1,10	122,710	124,226	-1,24	607,119	621,128	-2,31	1192,91	1242,26	-4,14
0,25	39,236	39,752	-1,32	78,141	79,504	-1,74	387,126	397,522	-2,69	763,929	795,043	-4,07
0,30	27,433	27,606	-0,63	54,113	55,211	-2,03	267,210	276,057	-3,31	528,601	552,113	-4,45
0,35	20,743	20,282	2,22	39,943	40,563	-1,55	194,876	202,817	-4,07	385,912	405,634	-5,11
0,40	17,014	16,618	2,33	31,232	31,056	0,56	148,100	155,282	-4,85	293,086	310,564	-5,96
0,45	15,205	15,149	0,37	25,923	24,538	5,34	116,362	122,692	-5,44	229,526	245,384	-6,91
0,50	14,683	14,699	-0,11	22,926	24,118	-5,20	94,147	99,380	-5,56	184,377	198,761	-7,80
0,55	14,994	14,952	0,28	21,557	22,646	-5,05	78,354	82,133	-4,82	151,406	164,265	-8,49
0,60	15,812	15,719	0,59	21,319	22,101	-3,67	67,139	69,014	-2,79	126,949	138,028	-8,73
0,65	16,925	16,882	0,25	21,829	22,244	-1,90	59,332	58,805	0,89	108,680	117,610	-8,22
0,70	18,202	18,368	-0,92	22,811	22,920	-0,48	54,132	50,704	6,33	95,104	101,409	-6,63
0,75	18,829	18,103	3,86	24,076	24,026	0,21	50,940	55,199	-8,36	85,156	88,338	-3,74
0,80	17,358	17,464	-0,61	25,502	25,492	0,04	49,273	52,387	-6,32	78,080	77,641	0,56
0,85	16,323	16,911	-3,61	27,009	27,271	-0,97	48,733	50,621	-3,88	73,283	68,775	6,15
0,90	15,624	16,426	-5,14	25,819	24,641	4,56	48,999	49,709	-1,45	70,273	75,158	-6,95
0,95	15,182	15,994	-5,35	24,086	23,848	0,99	49,820	49,511	0,62	68,638	71,817	-4,63
1,00	14,930	15,602	-4,50	22,769	23,140	-1,63	51,008	49,922	2,13	68,033	69,546	-2,22
1,05	14,816	15,242	-2,88	21,783	22,500	-3,29	52,424	50,865	2,97	68,177	68,181	-0,01
1,10	14,798	14,908	-0,75	21,056	21,915	-4,08	53,967	52,281	3,12	68,847	67,597	1,82
1,15	14,844	14,595	1,68	20,529	21,373	-4,11	55,566	54,127	2,59	69,872	67,698	3,11
1,20	14,927	14,297	4,22	20,154	20,866	-3,53	57,170	56,369	1,40	71,122	68,410	3,81
1,25	15,029	14,011	6,77	19,892	20,388	-2,49	58,742	58,983	-0,41	72,500	69,673	3,90
1,30	14,735	13,736	6,78	19,711	19,932	-1,12	55,377	50,916	8,06	73,936	71,445	3,37
1,35	14,120	13,467	4,62	19,585	19,494	0,47	52,050	49,369	5,15	75,377	73,689	2,24
1,40	13,597	13,203	2,89	19,495	19,070	2,18	49,179	47,917	2,56	76,784	76,381	0,52
1,45	13,149	12,944	1,56	19,424	18,657	3,95	46,692	46,545	0,32	78,130	79,502	-1,75
1,50	12,760	12,686	0,58	19,359	18,253	5,71	44,531	45,238	-1,59	77,385	69,456	10,25
1,55	12,420	12,430	-0,08	19,250	17,854	7,25	42,645	43,987	-3,15	72,838	67,292	7,61
1,60	12,116	12,173	-0,47	18,424	17,460	5,23	40,992	42,782	-4,37	68,795	65,232	5,18
1,65	11,841	11,916	-0,63	17,687	17,069	3,50	39,533	41,615	-5,27	65,190	63,259	2,96
1,70	11,587	11,658	-0,61	17,027	16,678	2,05	38,237	40,479	-5,86	61,964	61,361	0,97
1,75	11,348	11,398	-0,44	16,430	16,288	0,86	37,078	39,370	-6,18	59,068	59,526	-0,77
1,80	11,119	11,135	-0,15	15,887	15,897	-0,06	36,033	38,281	-6,24	56,459	57,744	-2,28
1,85	10,894	10,869	0,23	15,389	15,504	-0,75	35,083	37,209	-6,06	54,100	56,008	-3,53
1,90	10,672	10,601	0,66	14,929	15,109	-1,20	34,211	36,150	-5,67	51,958	54,309	-4,53
1,95	10,447	10,329	1,13	14,501	14,710	-1,44	33,404	35,102	-5,08	50,005	52,643	-5,28
2,00	10,168	10,054	1,12	14,100	14,309	-1,49	32,651	34,062	-4,32	48,217	51,004	-5,78